

Generic Roads to Neural Network Critical States

Ruedi Stoop and Karlis Kanders and Ralph Stoop

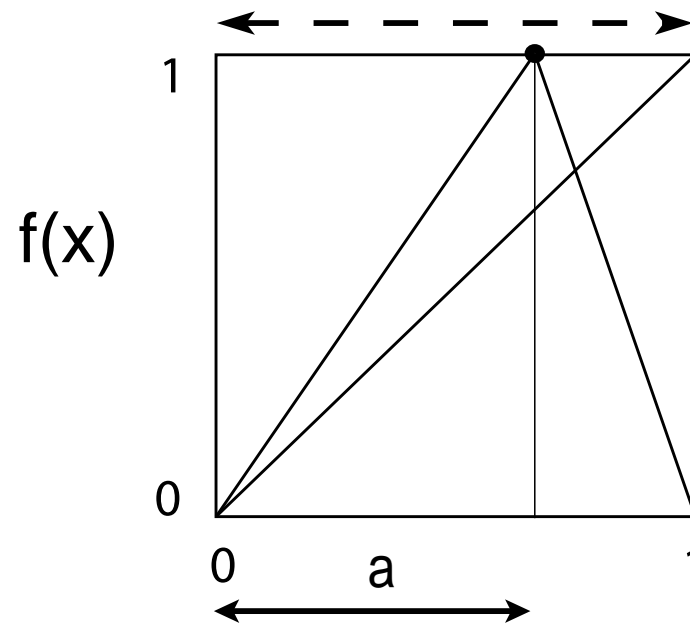
Institute of Neuroinformatics UNI / ETH of Zurich



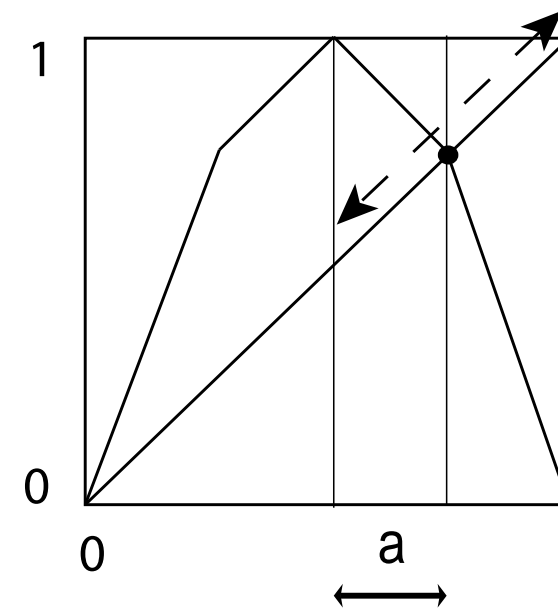
'Information' in the nervous system

- 'external' impulses: information sent out to trigger: exponential decay in time
- 'internally retained information': dynamically stored information, e.g. containing the form of the trigger (words): slower than exponential decay is required
- (not considering chemically stored information)

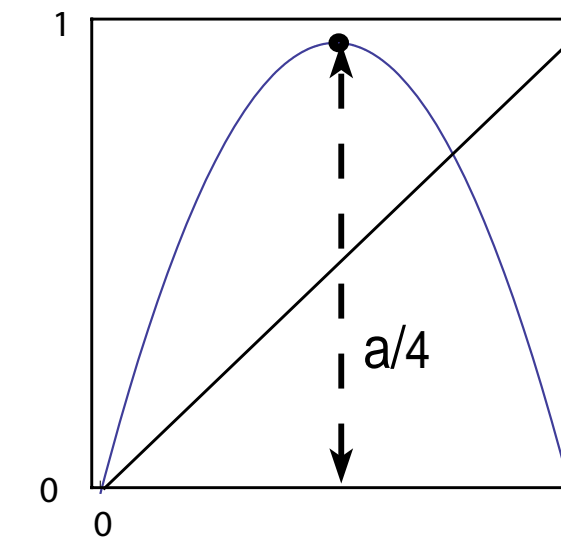
Typical dynamical systems (information: initial condition):



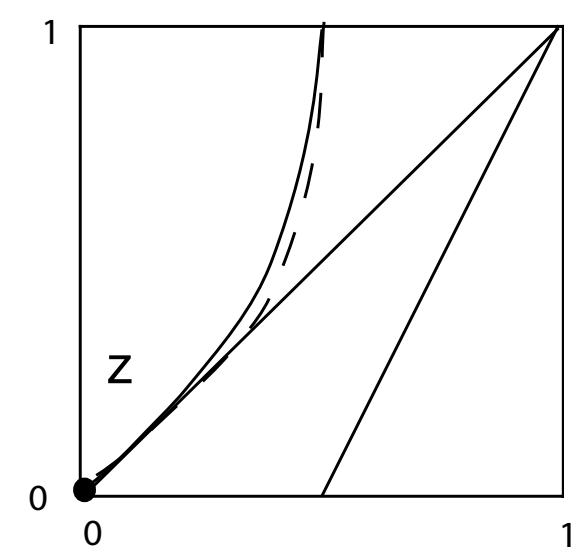
exponential



exponential



nonhyperbolic
exponential

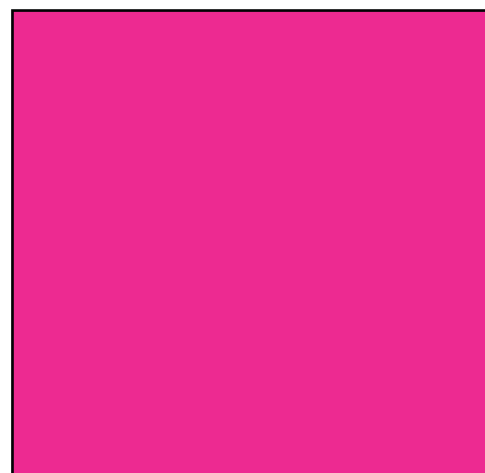


nonhyperbolic
nonexponential

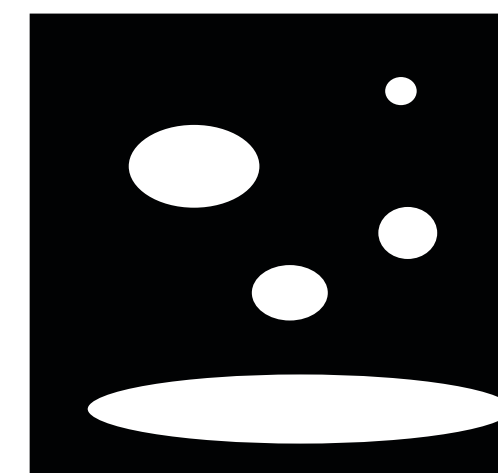
time to space conversion

- sequential state update along trajectory

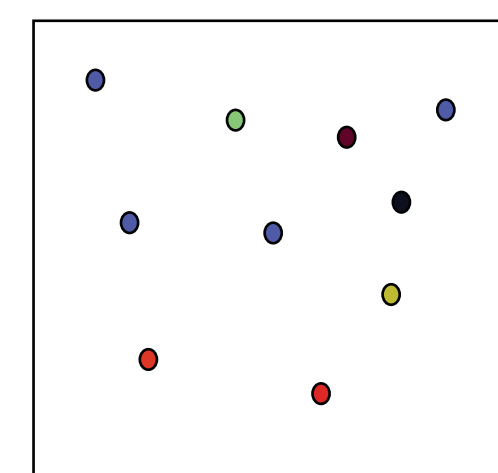
I



II



III



'frozen'
system does not
change

patterns of all sizes

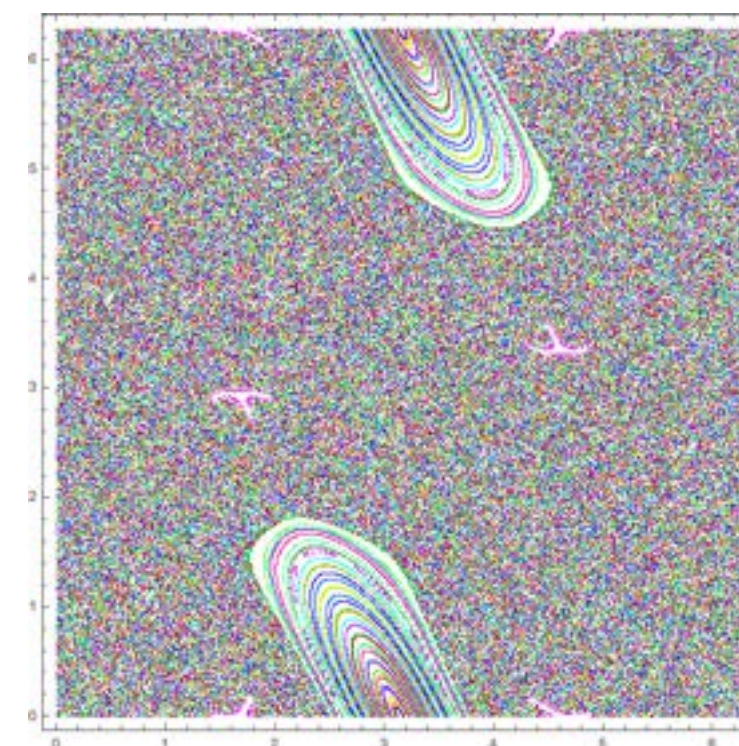
system forgets

III: 'critical' system state, states clearly distinguished (e.g. by transfer operator spectrum)

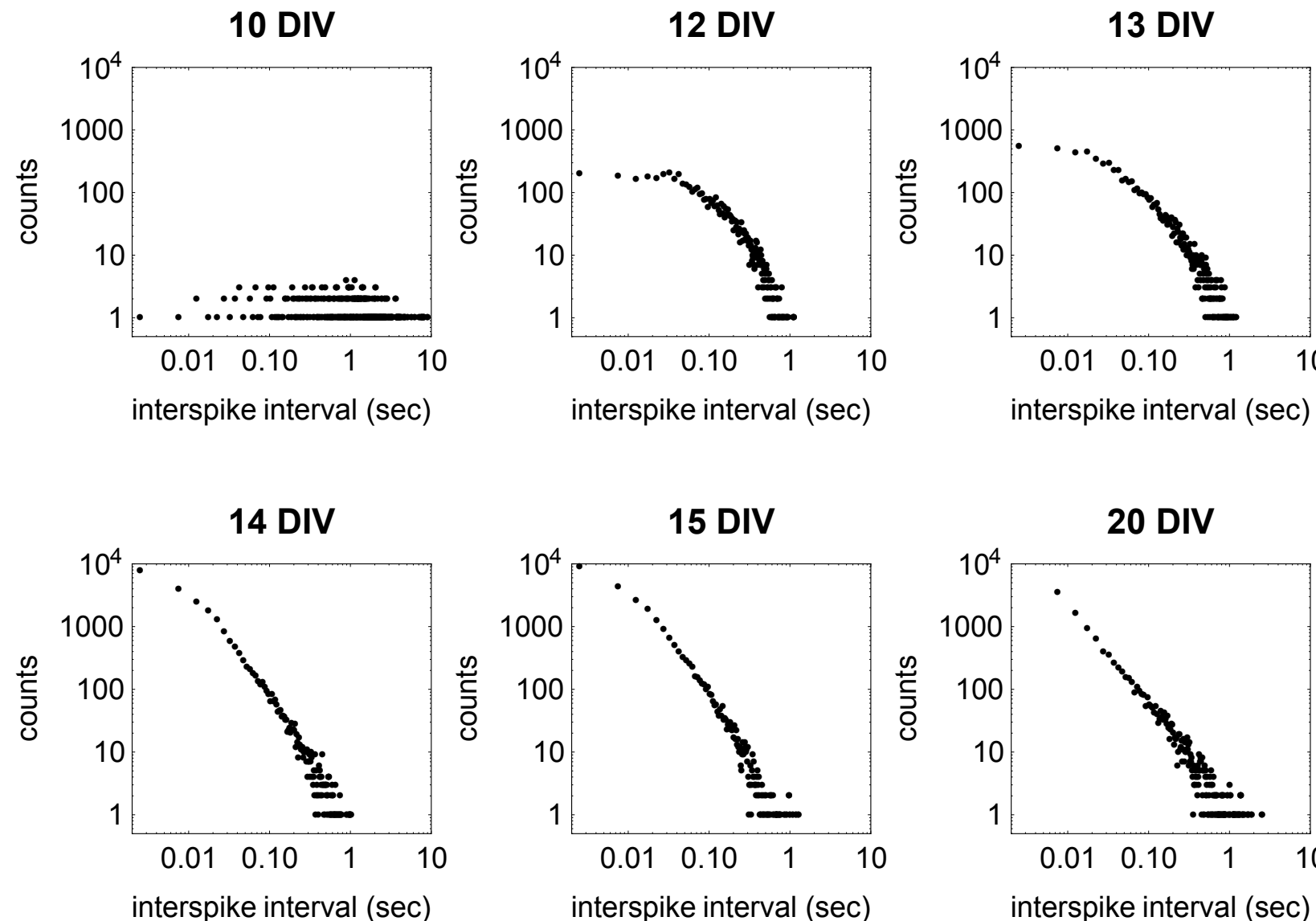
properties

- optimal state for living systems
(‘edge of chaos’, D.Farmer, C.Langton)
- dynamically: chaos in dynamical sense: zero Lyapunov exponent, but system has memory, can be unstable & complex
known: often: power-law distributed values of finite-time LE with distinct power-law exponents (we do not consider ‘self-organized criticality universality’)
- topologically: if states are associated with ‘active’ and ‘silent’, we obtain ‘firing avalanches’: firing sequences of all sizes, with power-law distributed probabilities

Are these characterizations always the same?
If not: Are there simple examples?

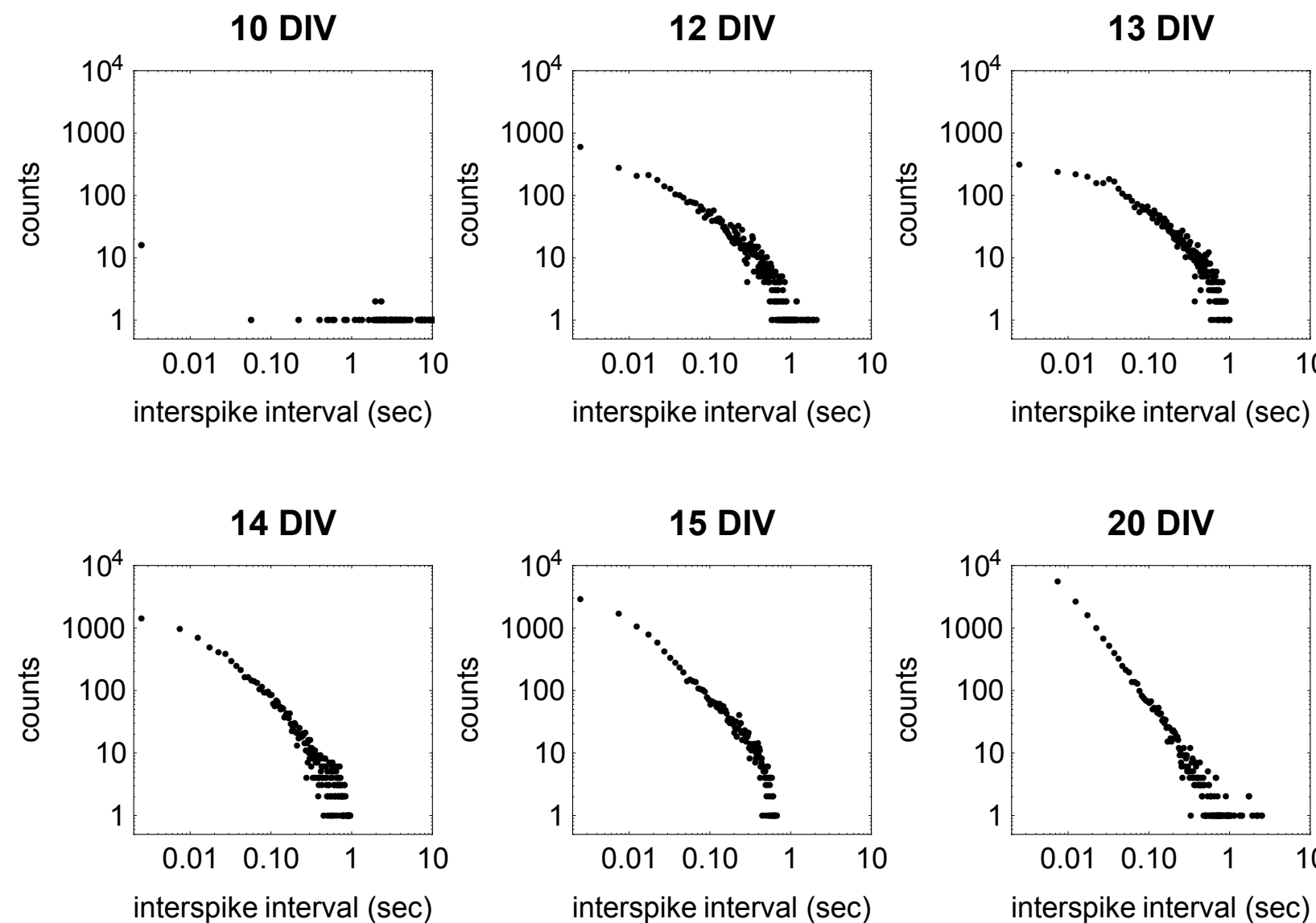


hypocampal neuronal culture development



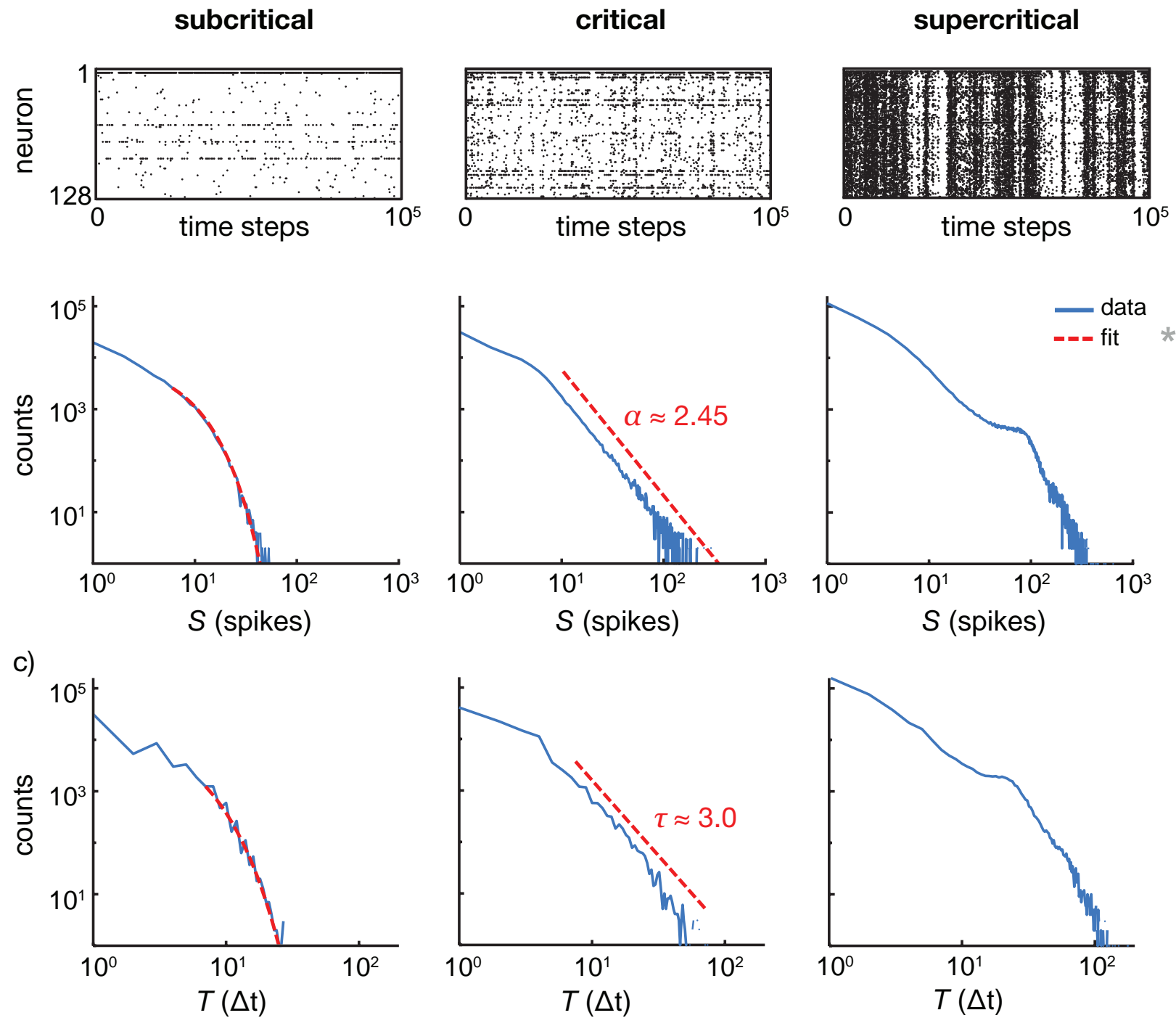
Transformation shape of interspike interval distributions: exponential (DIV 12-13) towards power-law (DIV 14-15, 20). Power-law slope: 1.75 (DIV) 14-15, and 1.6 (DIV 20).

culture development



Transformation shape of interspike interval distribution: exponential (DIV 12-13) towards power-law (DIV 14-15, 20). Power-law slope: 1.75 (DIV) 14-15, and 1.6 (DIV 20). 800 cells mm².

culture development



weak synapses

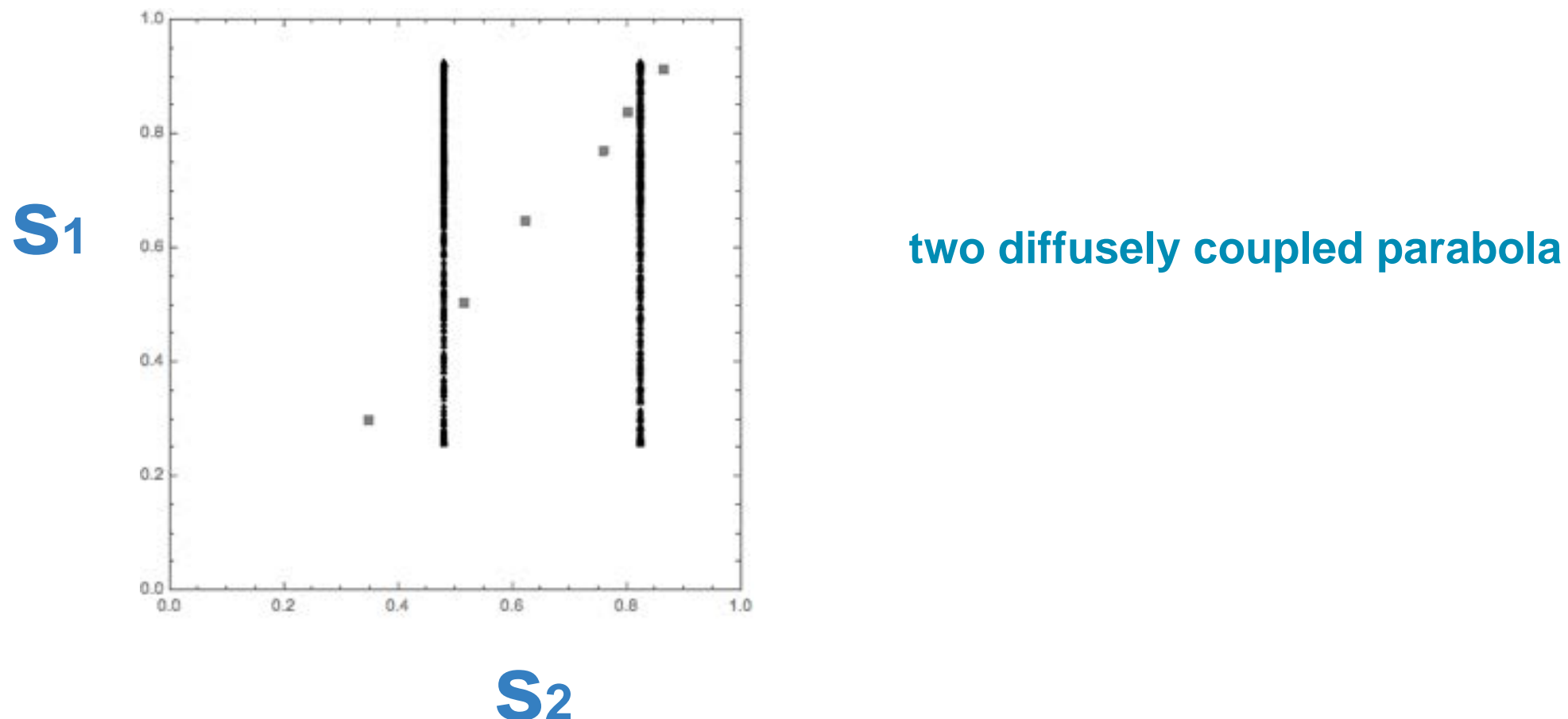
strong synapses

*humps: Lorimer, Gomez, Stoop, Sci. Rep., 2015

testing criticality co-occurrence hypothesis

Caveats:

1) *coupled systems often deviate from the nature of the constituents*





2) **Critical states do not exist in nature**

finite size problem (no thermodynamic limit)

biology:

- **open systems (they react upon external input)**

several levels of hierarchies

at each level of the hierarchy, ‘whatever architecture works’ is used - non-scaling

Approximative scaling approach

consider scaling only across the range directly related to the scale of the model

(in what follows: cortical columns)

**cortical hierarchy can display properties ascribed to critical systems nonetheless,
if each hierarchy level optimizes its behavior at its own level**

We call states ‘critical’, if they sufficiently share (topologically or dynamically) the statistical properties of finite size states of systems close to a (provable) critical point.

Such properties are:

- scaling within system size

- relations between critical exponents



Scaling Brain Size, Keeping Timing: Evolutionary Preservation of Brain Rhythms

Gyorgy Buzsaki,^{1,*} Nikos Logothetis,² and Wolf Singer³

¹The Neuroscience Institute, Center for Neural Science, School of Medicine, New York University, New York, NY 10016, USA

²Max Planck Institute for Biological Cybernetics, Tübingen, Germany; Imaging Science and Biomedical Engineering, University of Manchester, Manchester, UK

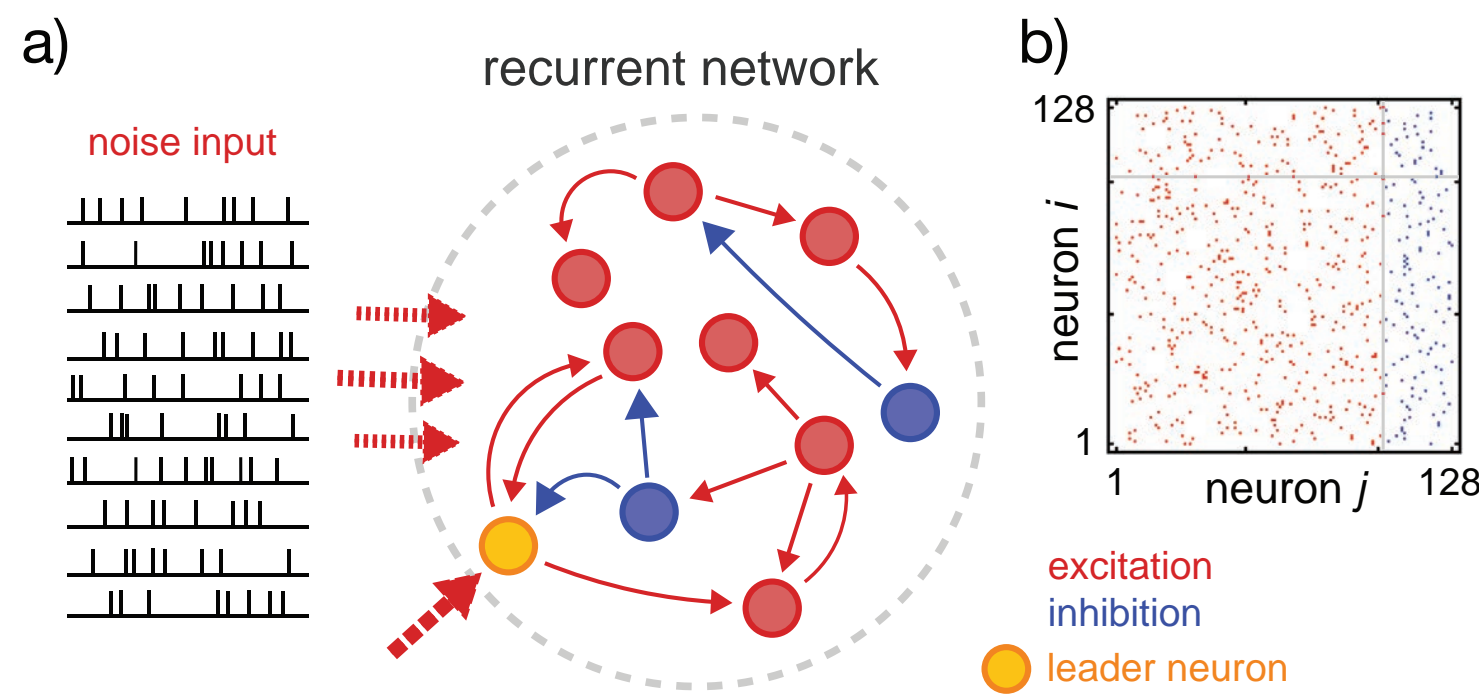
³Max Planck Institute for Brain Research (MPI), Ernst Struengmann Institute for Neuroscience in Cooperation with the Max Planck Society, Frankfurt Institute for Advanced Studies, Frankfurt am Main, Germany

Despite the several-thousand-fold increase of brain volume during the course of mammalian evolution, the hierarchy of brain oscillations remains remarkably preserved, allowing for multiple-time-scale communication within and across neuronal networks at approximately the same speed, irrespective of brain size. Deployment of large-diameter axons of long-range neurons could be a key factor in the preserved time management in growing brains. We discuss the consequences of such preserved network constellation in mental disease, drug discovery, and interventional therapies.

strategy

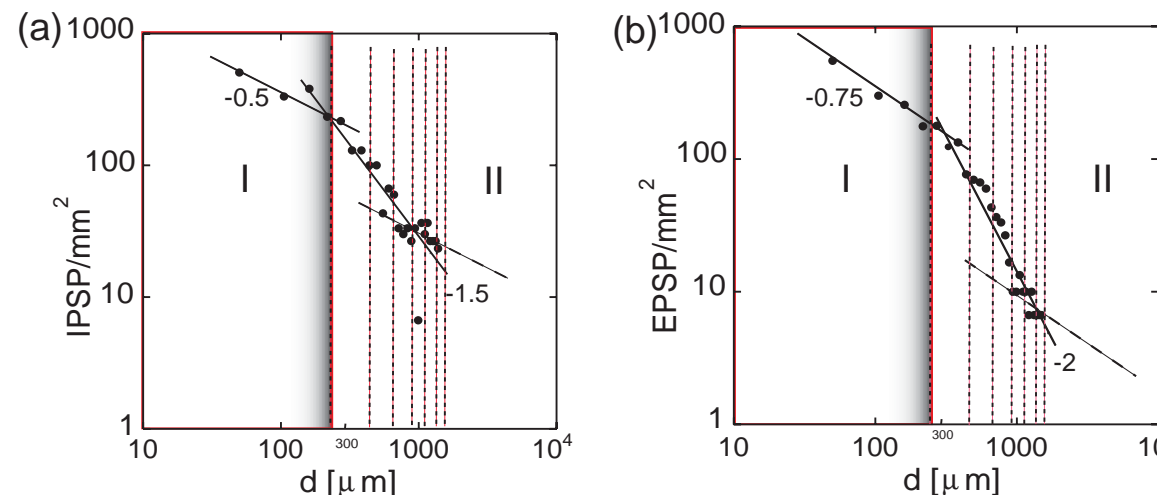
- counter-example: suffices: one system, one parameter set (Chaos 27, 047408, 2017)
- genericity: ensembles, parameter intervals, if possible intrinsic explaining arguments

model: cortical column



- a) Recurrent network with excitatory neurons (red circles), inhibitory neurons (blue circles) and intrinsically firing excitatory neurons (yellow circles) representing entrant sensory stimulation. Each neuron also receives noisy excitatory input, from a Poisson spike train
- b) Weight matrix w of the network, with excitatory connections (red) and inhibitory connections (blue). Grey lines are for the last excitatory neuron (index $j = 102$)

known connectivity:



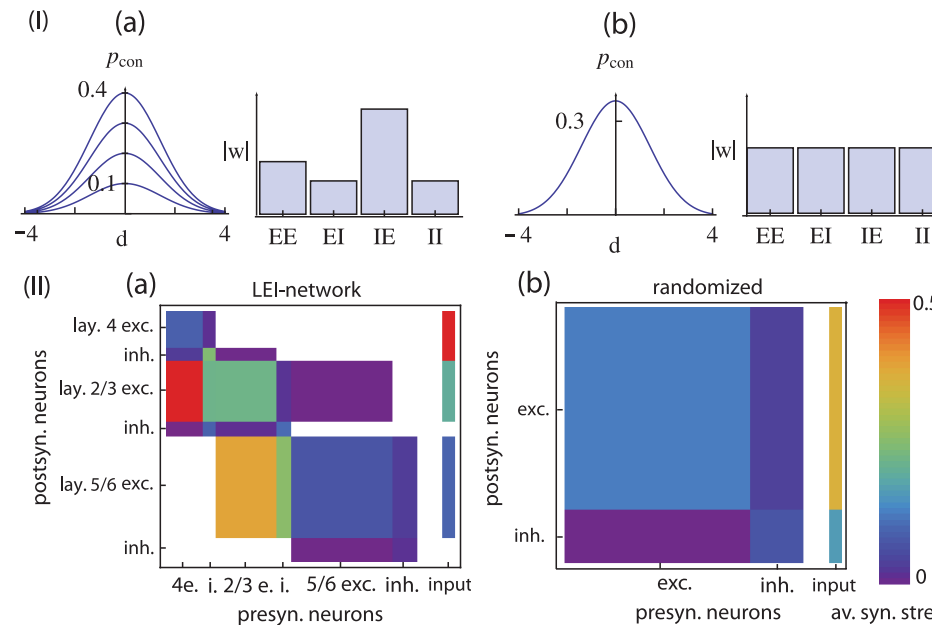
Ferret striate cortex (adaptation from Röhricht et al.):

Log-density of photostimulation-evoked excitatory (a) and inhibitory (b) synaptic inputs

(concentric rings 50 μm apart, from 19 pooled layer 2/3 neurons).

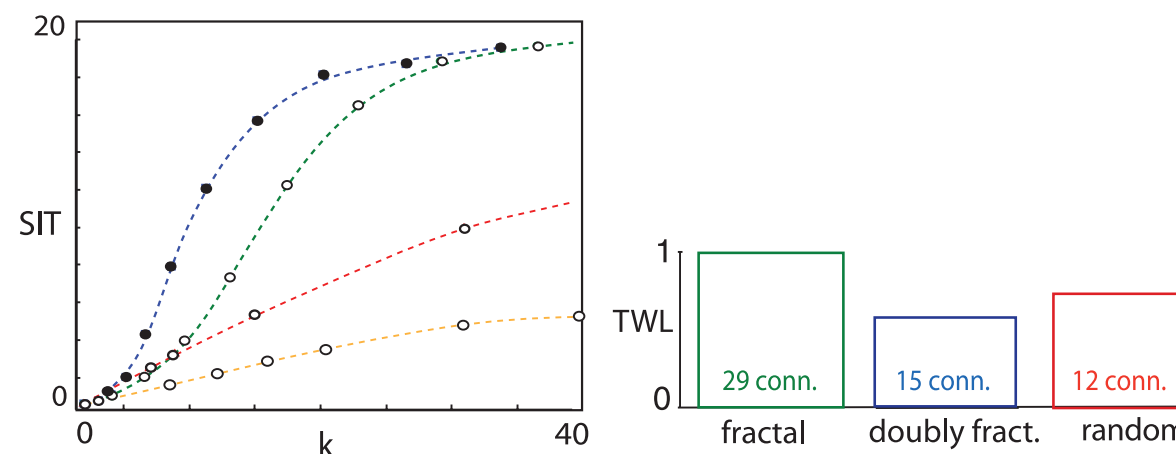
(I): Inner-columnar, (II): Intercolumnar scale. Vertical lines: Extensions of aligned physiological columns.

Tilted dashed lines: Proposed long distance decay.



- **reservoir computing**
- **microcircuits irrelevant!**
- **PRL 2013**

known connectivity:



Speed-of-information-transfer SIT:

From top:

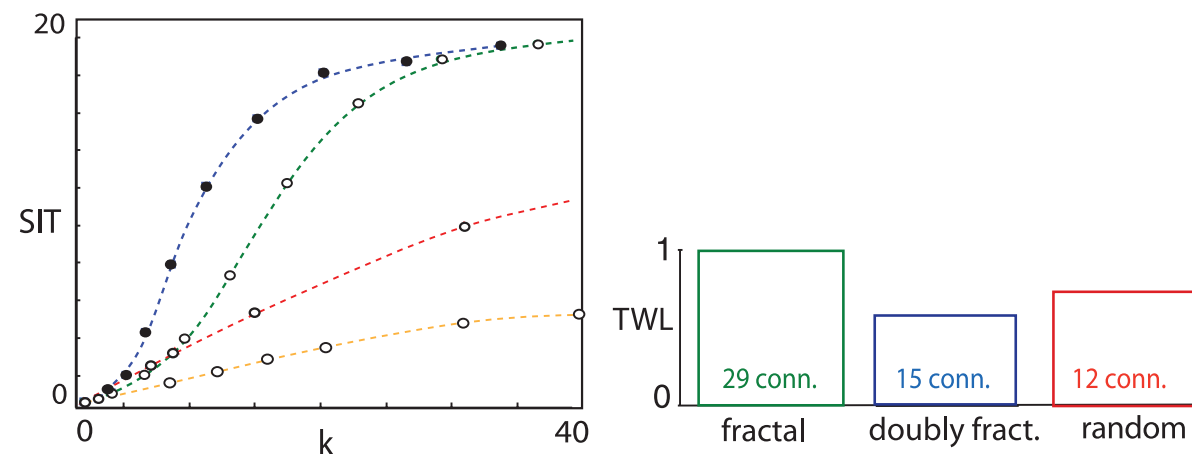
doubly fractal, fractal, random, n.-n. topology.

Network sizes: 4096, averages over 100 experiments.

Right: Connections k_{min} required for synchronization, and associated TWL.

: columnar structures may express a sufficient (but not necessary) facilitating structure for a combined SIT/TWL optimization!

neuronal cultures:



Speed-of-information-transfer SIT:

From top:

doubly fractal, fractal, random, n.-n. topology.
Network sizes: 4096, averages over 100 experiments.
Right: Connections k_{\min} required for synchronization, and associated TWL.

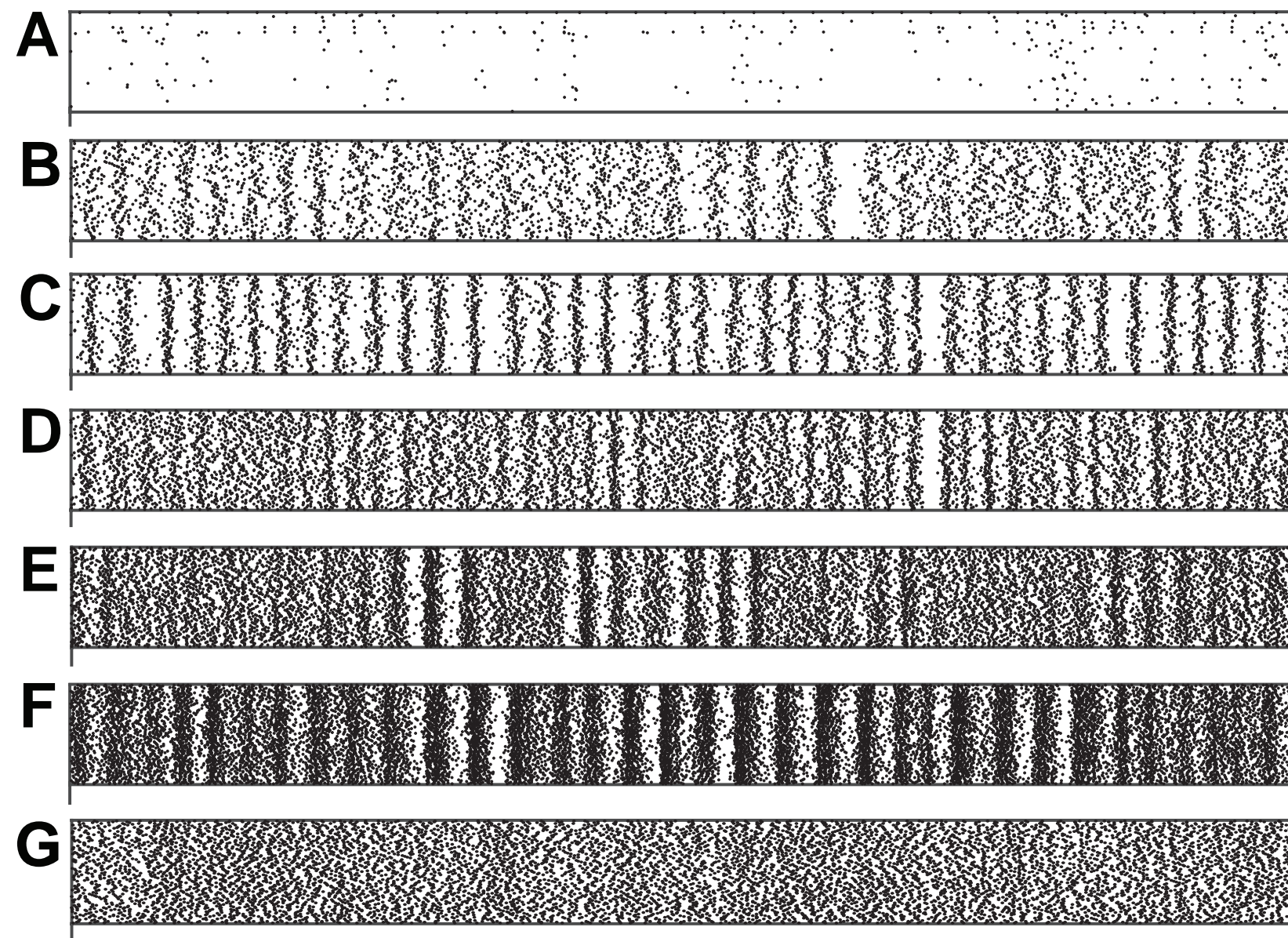
elements:

- network built on a network graph, with Rulkov model neurons as nodes
- size: 32-256 (centered around cortical column size 128)
- 1: 4 part composition of inhibitory vs. excitatory neurons
- connectivity probability of $p_c = 0.04$
- construction: in-degree 4-5, out-degree variable
- Rulkov neurons initially below threshold
- leader neurons, representing incoming information above firing threshold; subtly chaotically firing
- noise input temporally sparse
- synaptic dynamics (mesoscopic synapses, inhibitory synapses by a factor around 3 stronger):

$$I_{n+1}^{(i)} = \eta I_n^{(i)} + W \left(\sum_{j=1}^{N_{ex}} w_{ij} (x_{rp}^{ex} - x_n^{(i)}) \xi_n^{(j)} + \sum_{j=N_{ex}+1}^N w_{ij} (x_{rp}^{inh} - x_n^{(i)}) \xi_n^{(j)} + w_{ext} (x_{rp}^{ex} - x_n^{(i)}) \xi_n^{ext(i)} \right).$$

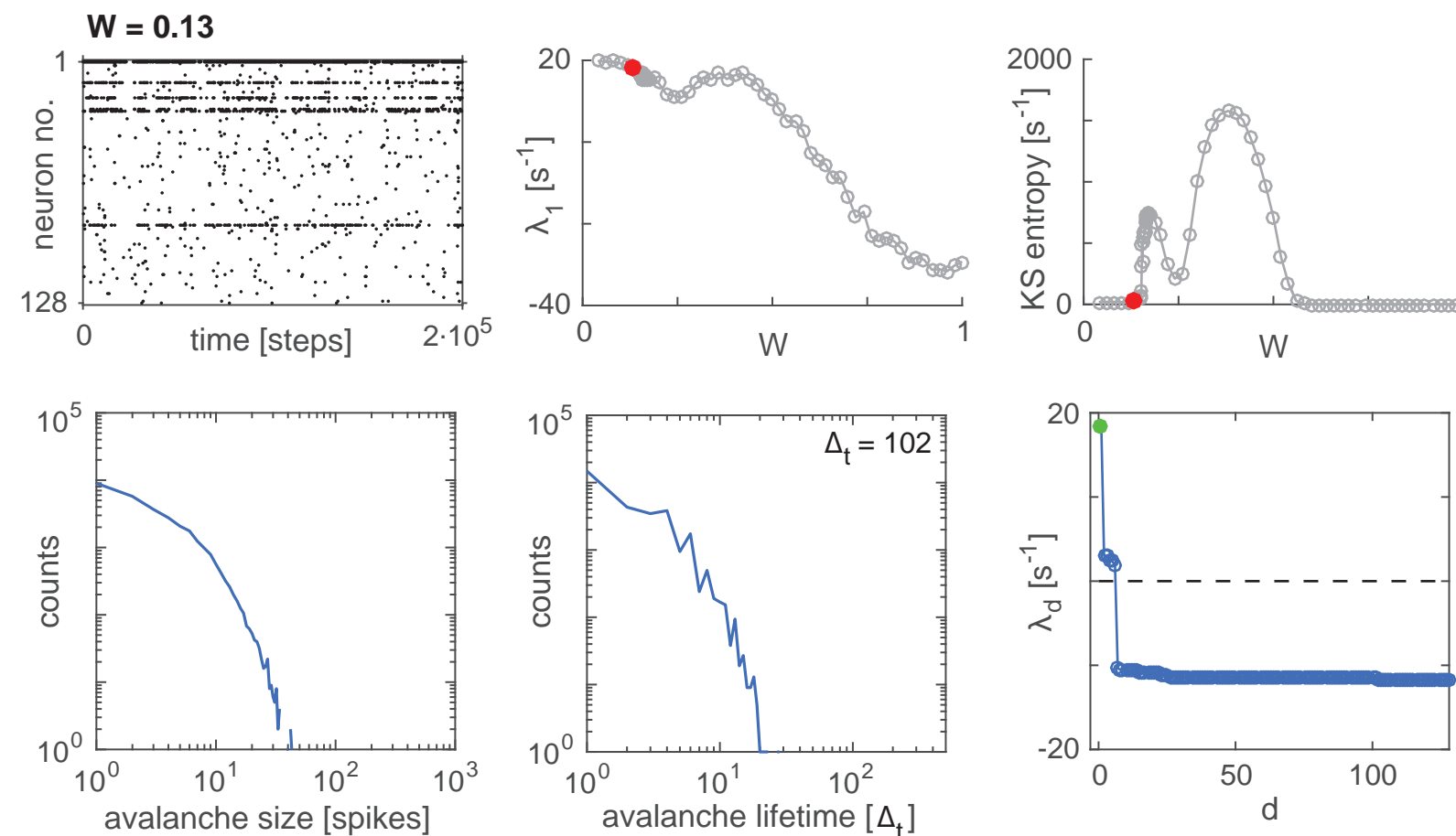


typical behavior upon changing W:



Firing behavior for $W = 0.14, 0.18, 0.24, 0.34, 0.44, 0.54, 0.9$, from top to bottom.
Rasterplots; vertical axis: neuron number, horizontal axis: time (A-F: 10000, G: 2000 time steps).

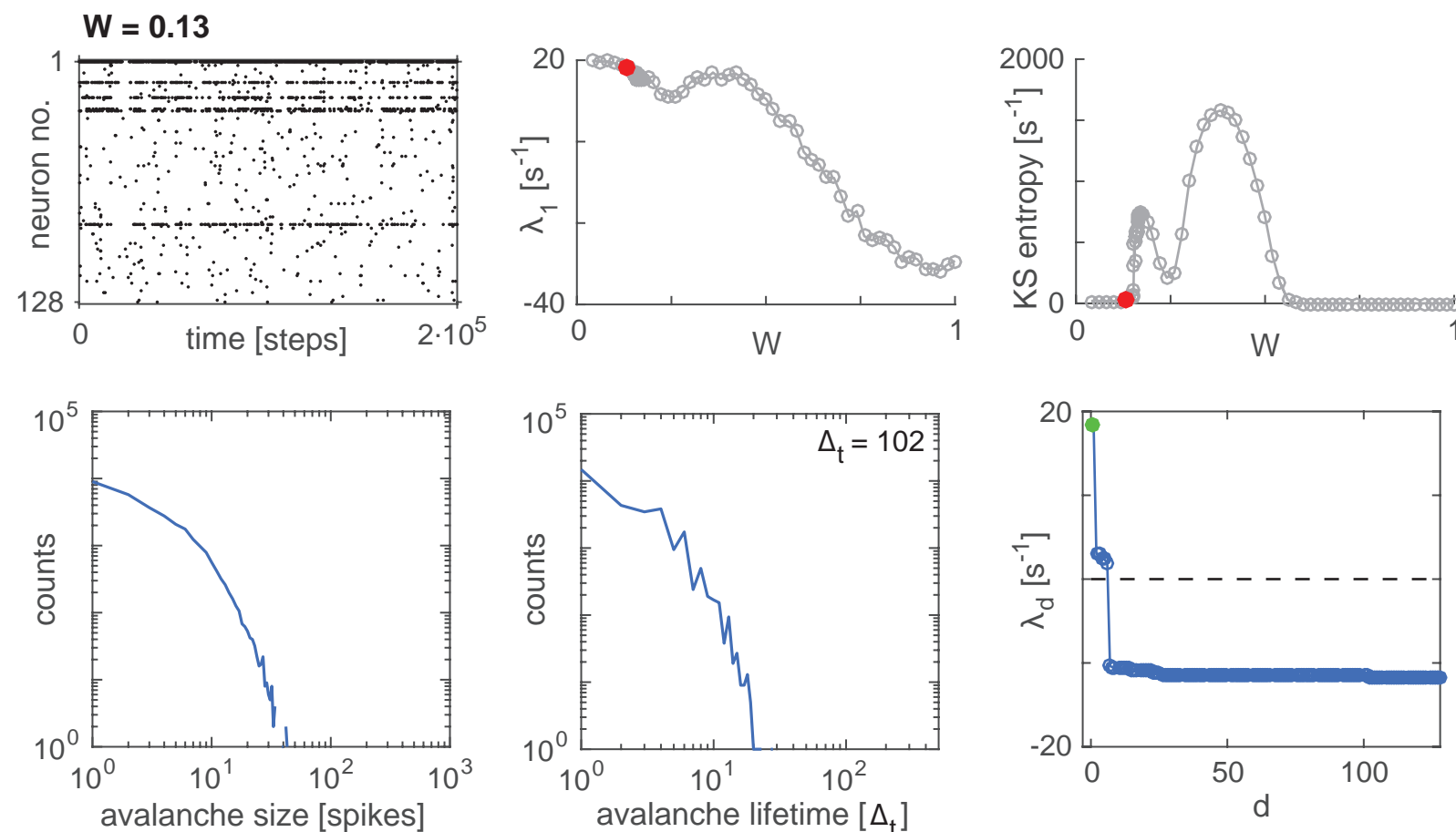
W=0.12



Up to avalanche criticality, overall firing activity remains at an almost unchanged level.
Lifetime-distribution reflects of the presence of a leader neuron.

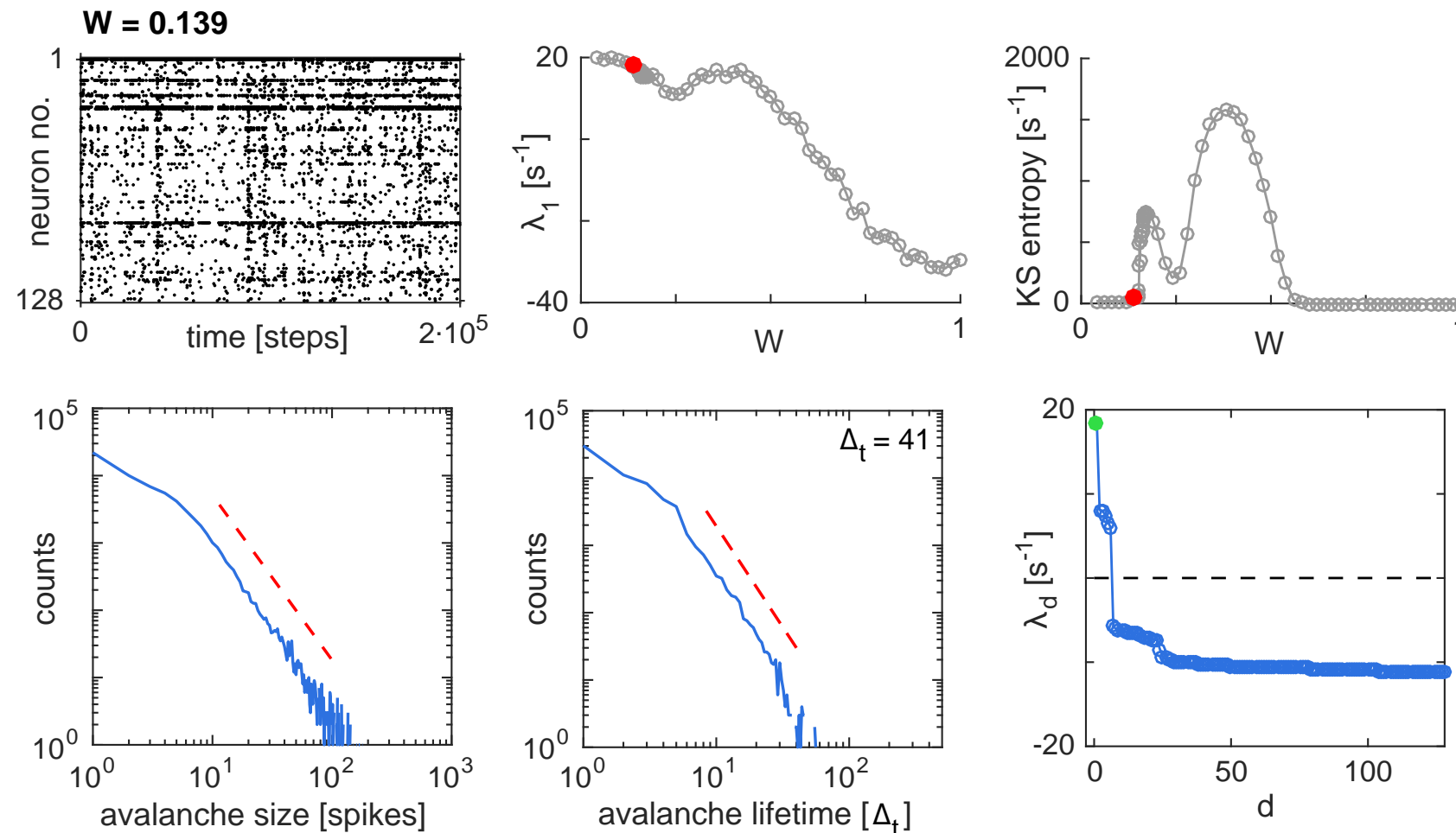


W=0.13



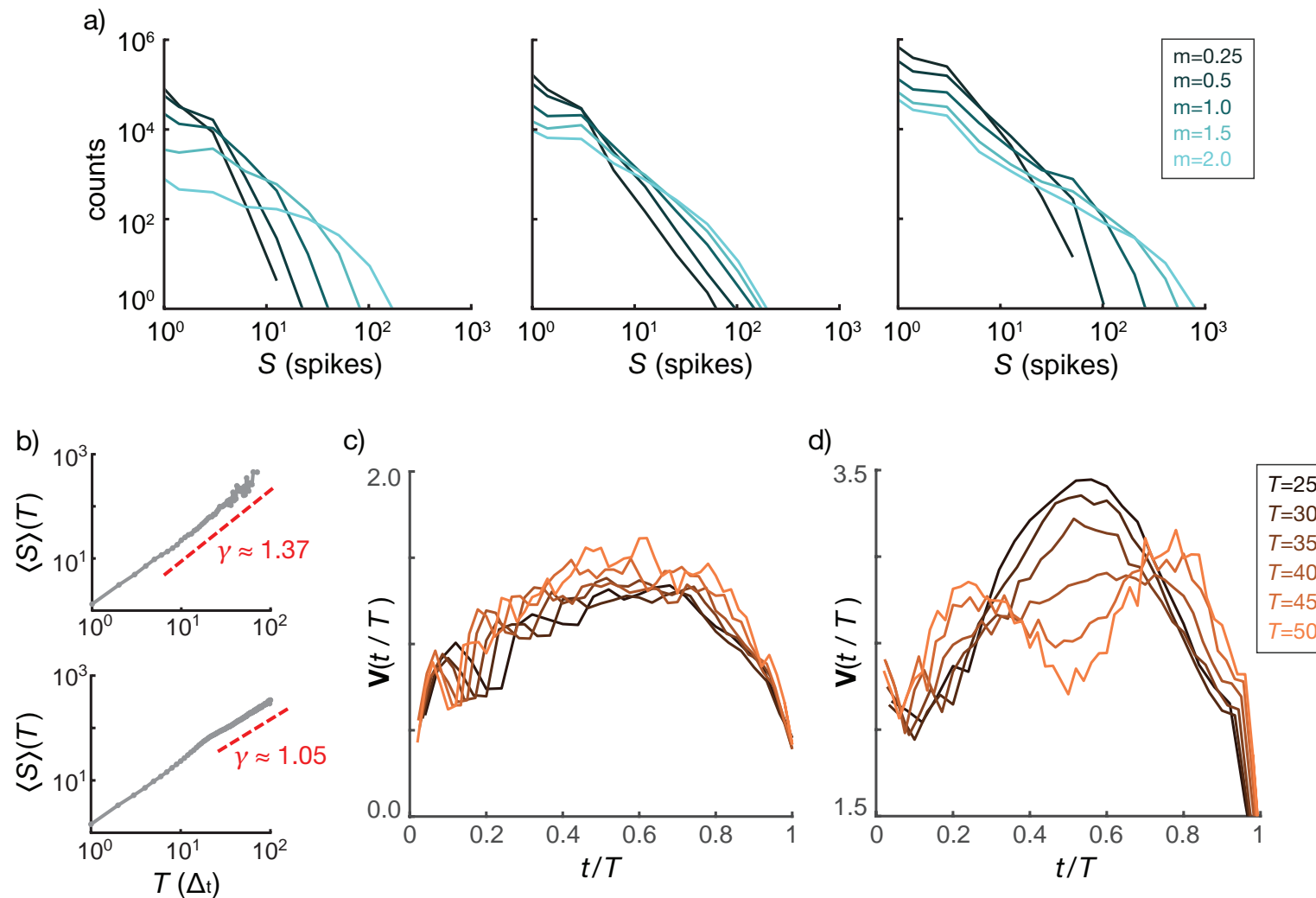
Towards avalanche criticality: At $W = 0.13$, additional modes become unstable

$W=0.139$: Avalanche critical point



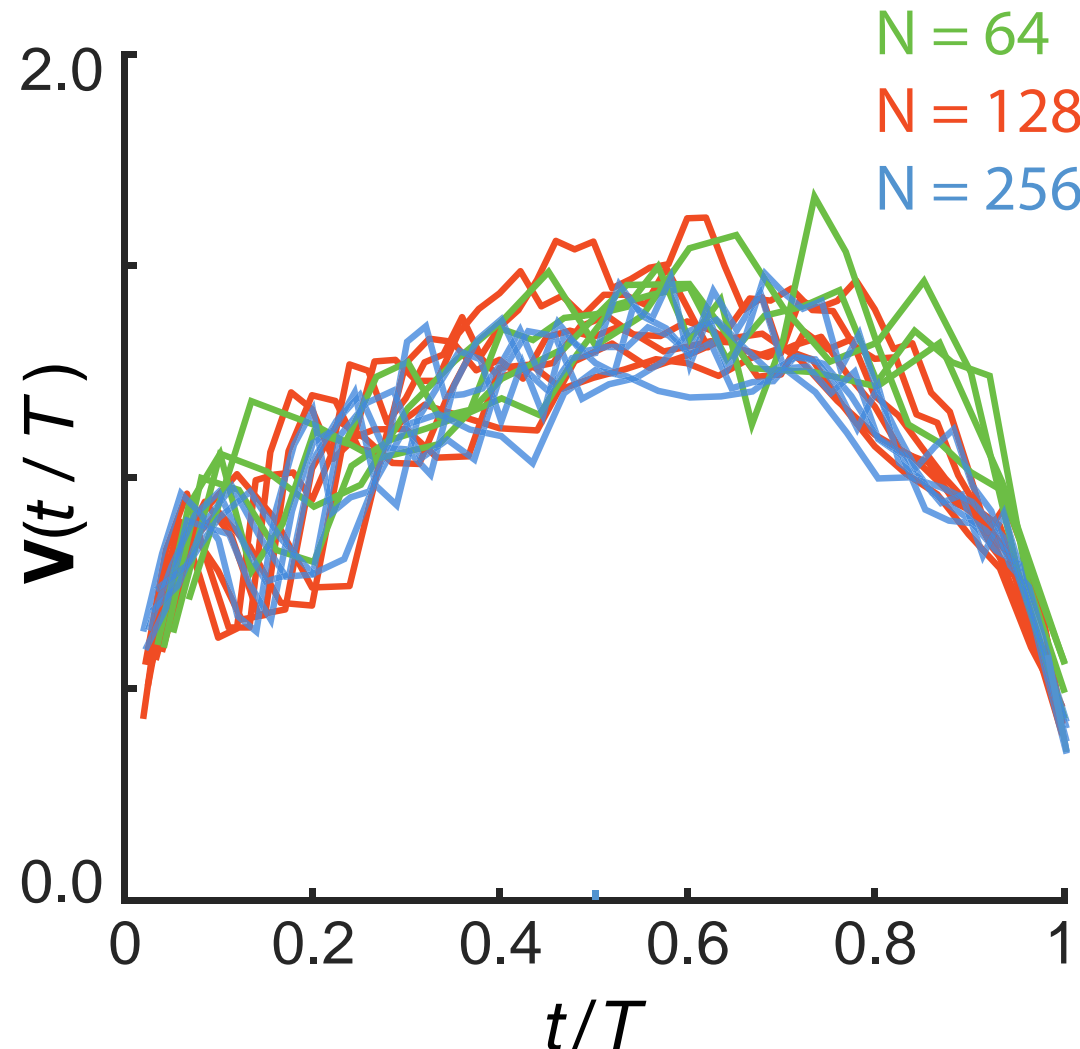
At avalanche criticality ($W = 0.139$), an avalanche size power-law decay exponent of $\alpha \approx 2.45$ is obtained, using Beggs and Plenz's method

criticality tests



- a) Avalanche size distributions based on time bins of size $\tilde{\Delta}_t = m \cdot \langle IEI \rangle$, $m \in \{0.25, 0.5, 1.0, 1.5, 2.0\}$, for subcritical (left, $W = 0.13$), critical (middle, $W = 0.139$), and supercritical states (right, $W = 0.15$), logarithmic histogram binning.
 b) Mean avalanche size as a function of lifetime, for critical (top) and supercritical (bottom) states.
 The red dashed line: power law relationship $\langle S \rangle(T) \propto T^\gamma$.
 c) Avalanche shapes of the critical state show a noisy collapse ($T \in \{25, 30, \dots, 50\}$, from darker to lighter), expressing a high degree of self-similarity, but also the particular role of the intrinsically firing neuron neurons.
 d) For the supercritical state, rescaling does not lead to a collapse ($T \in \{25, 30, \dots, 50\}$).

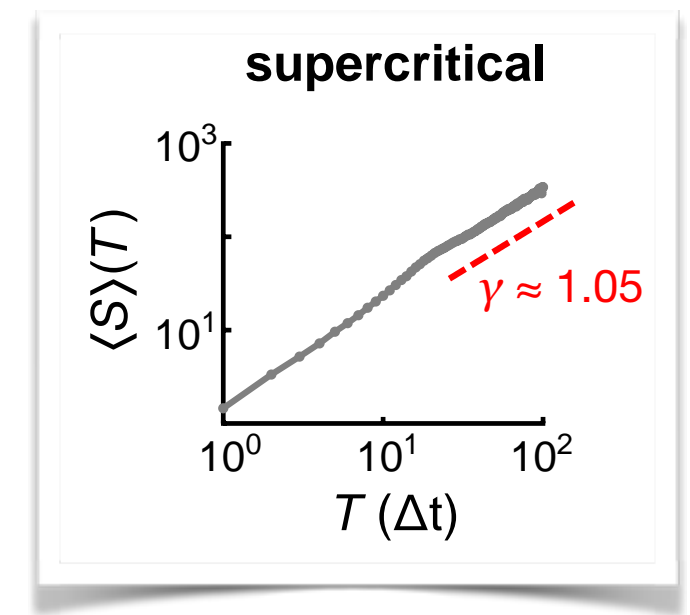
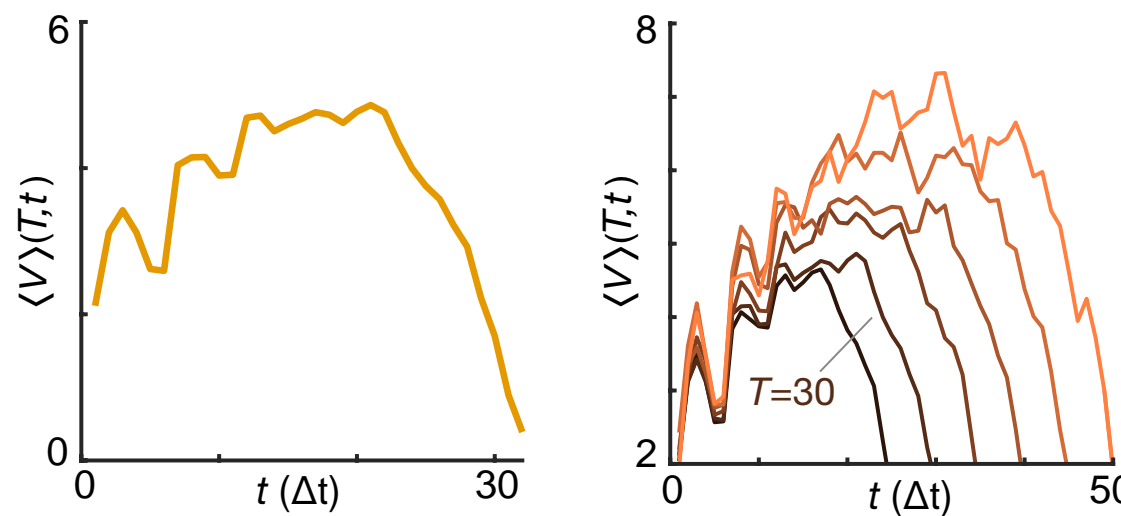
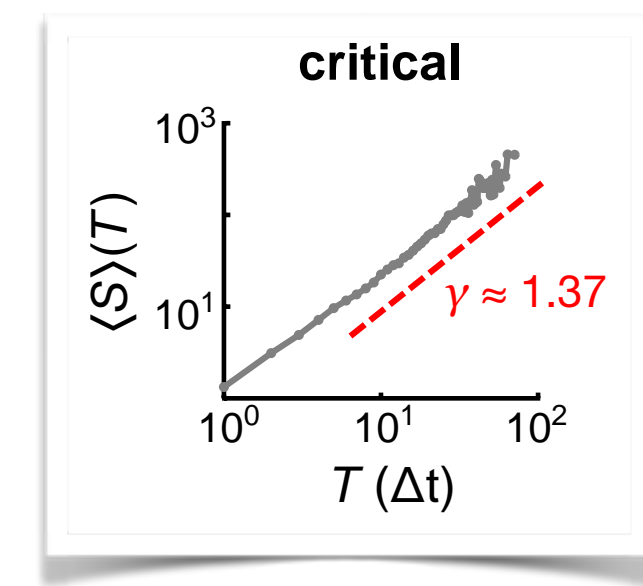
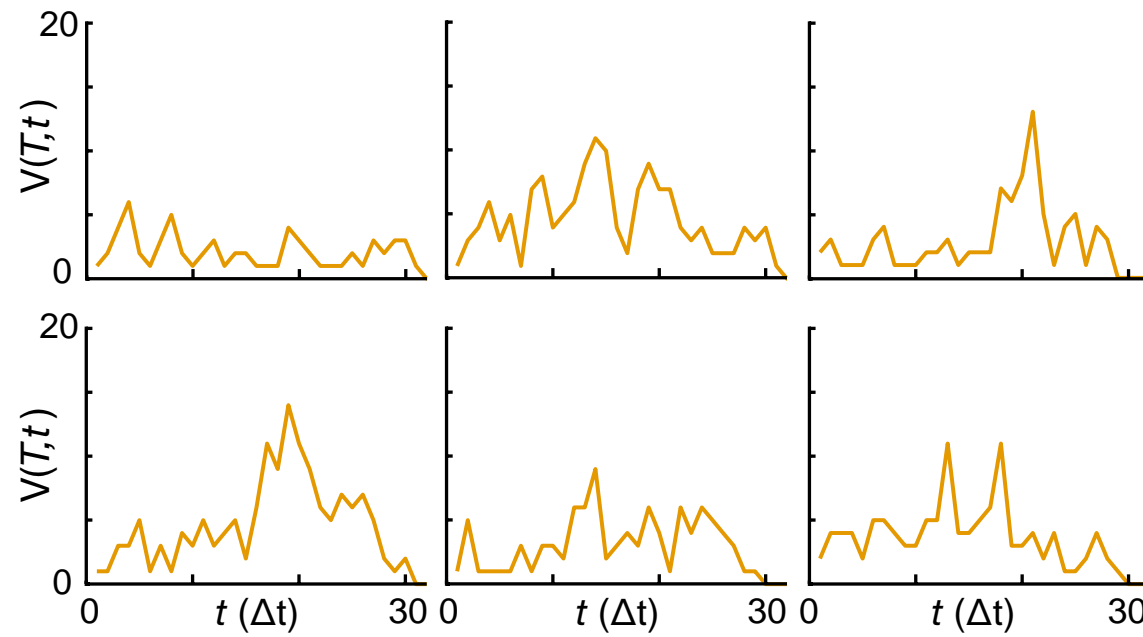
criticality tests



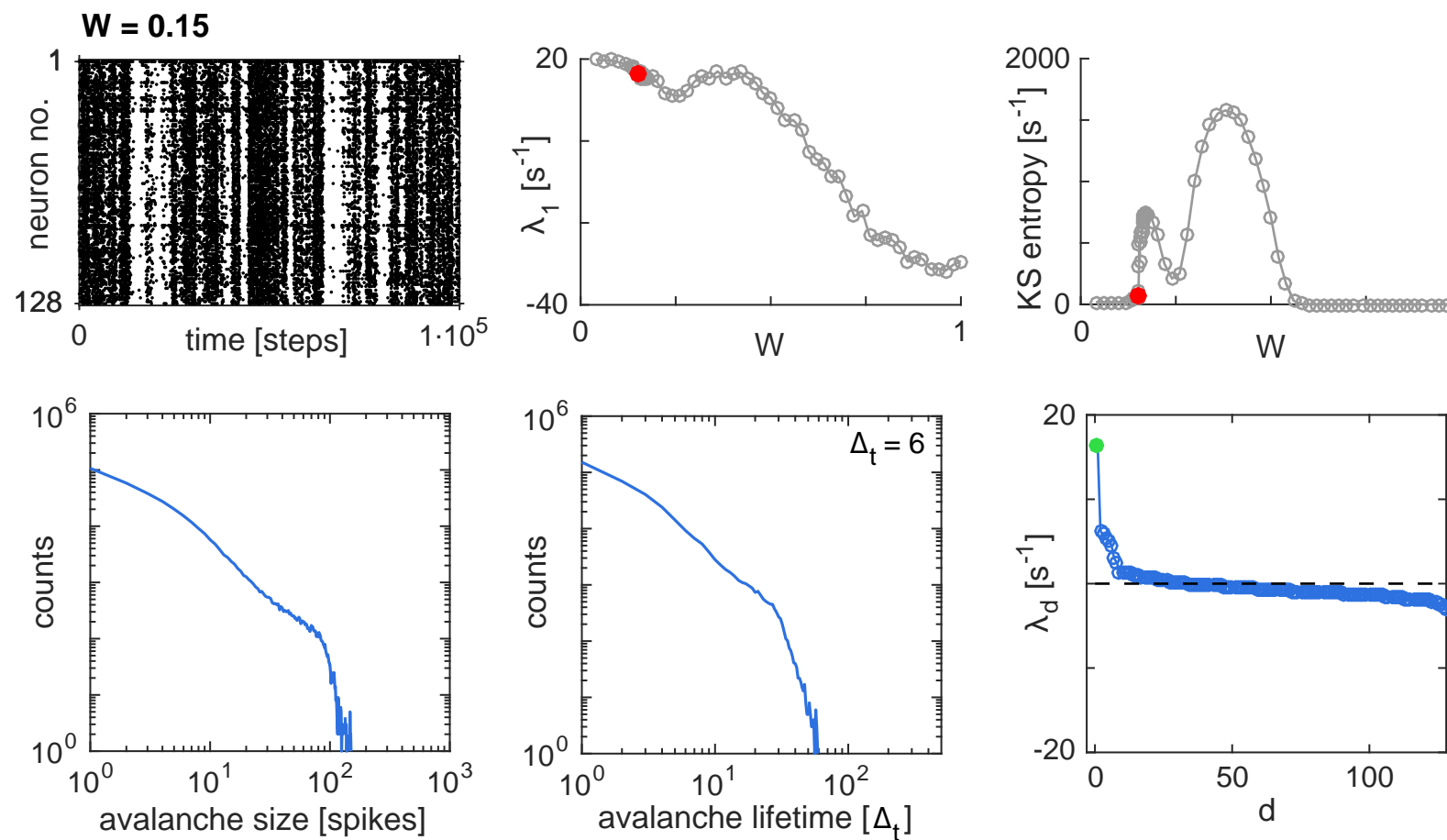
Scaling in system size L across the columnar scale, with N denoting the number of neurons in the network.
Our results for $N \in \{64, 128, 256\}$ collapse.
Beyond this range, strongly outside of the columnar scale, an appropriate scaling of the connectivity
(and of the number of nucleation sites) would need to be provided, which is non-biological.

Universal scaling function

$$\mathbf{V}(t/T) = T^{1-\gamma} \langle V \rangle(T, t/T)$$

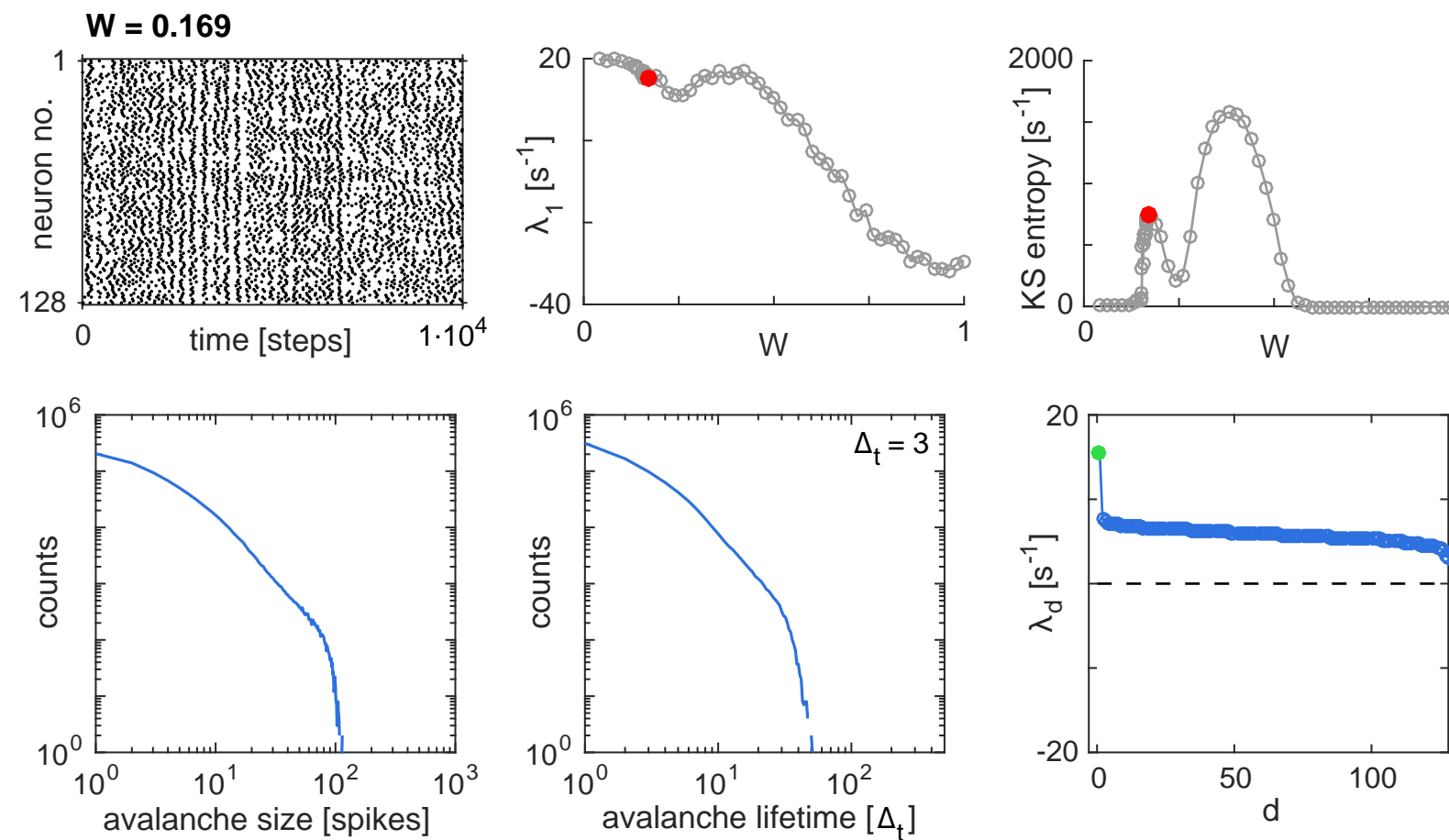


$W=0.15$: Beyond avalanche critical point: multiple transformations



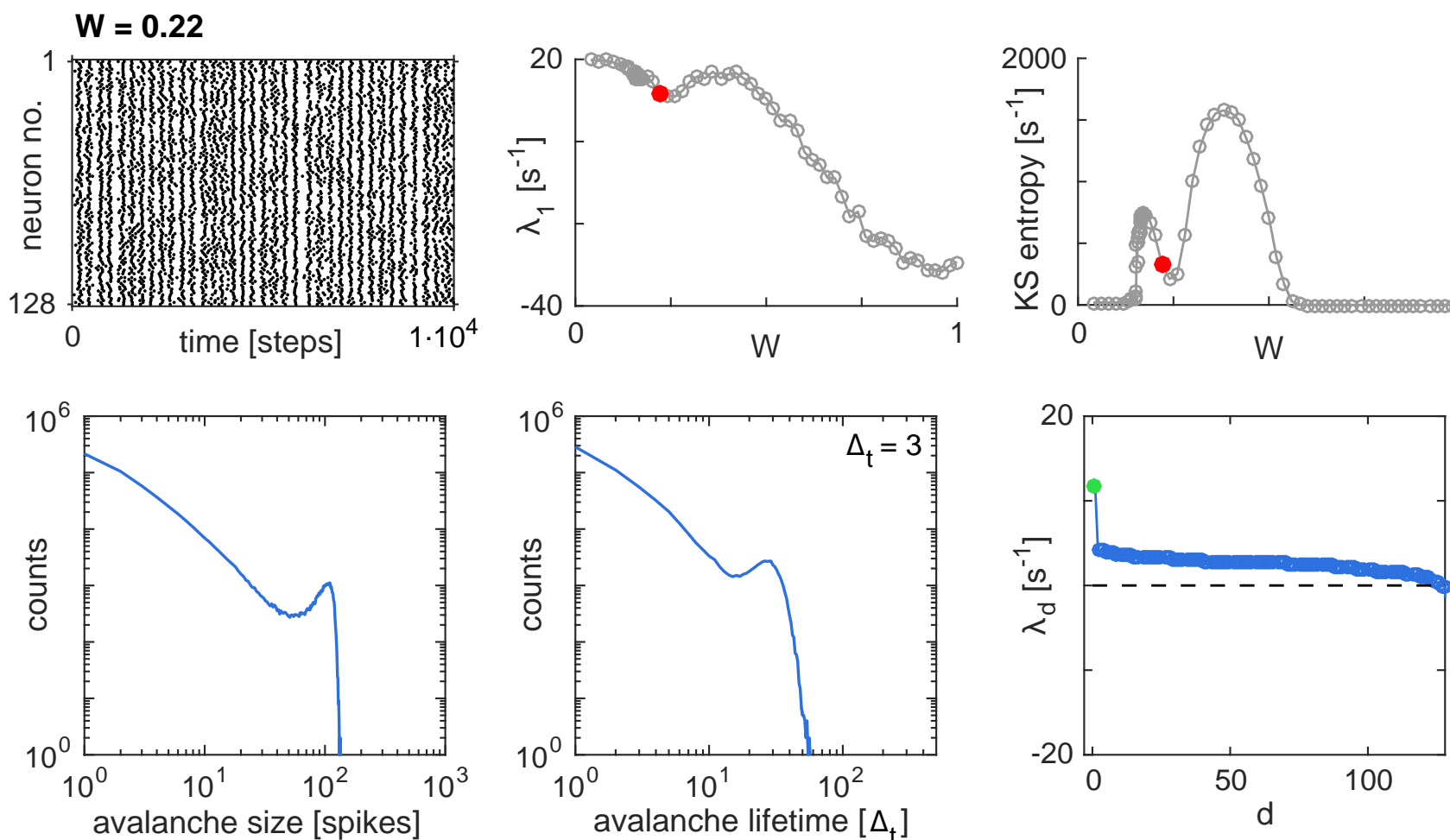
After avalanche criticality, we observe a rather abrupt increase in firing activity, as could be expected from an order parameter in the vicinity of a critical state. The strong increase continues up to $W = 0.15$; at higher values $0.15 < W < 0.6$, the increase with W becomes more moderate.

W=0.169



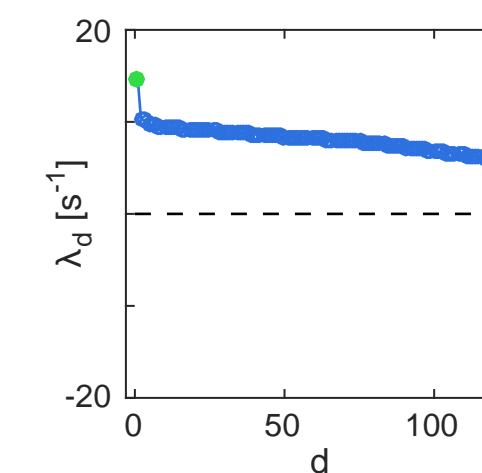
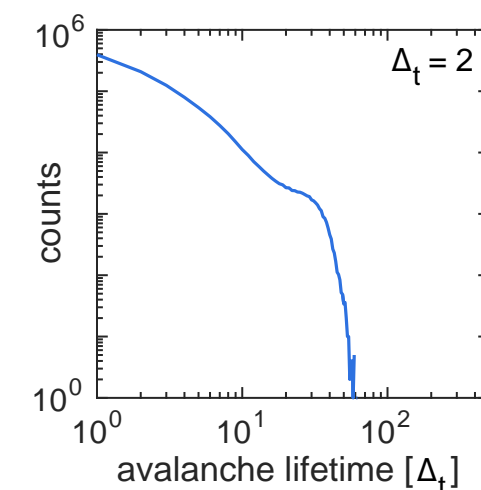
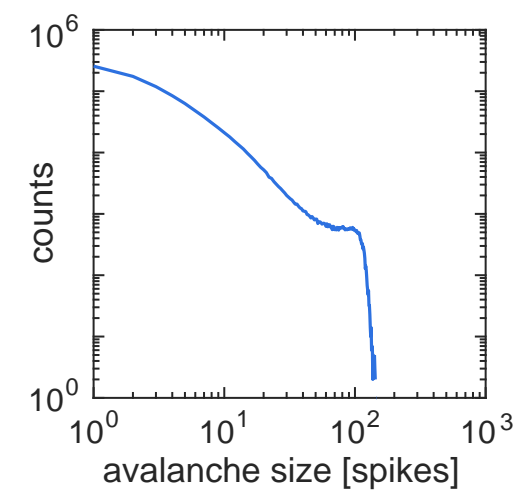
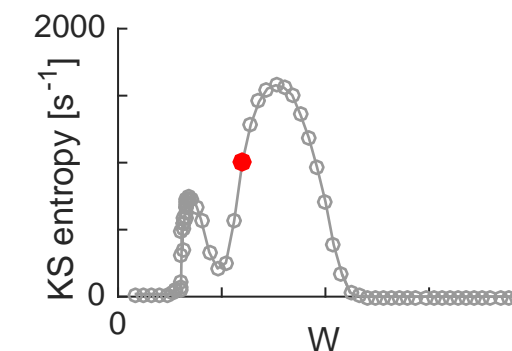
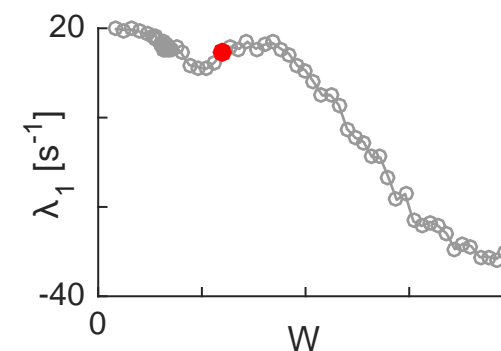
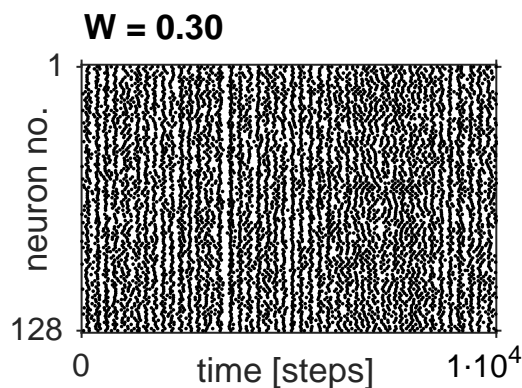
First local maximum of the Kolmogorov-Sinai entropy, based on temporally extended firing patterns.
Although the distributions have a faint power-law appearance, the data is not invariant to binning.

W=0.22



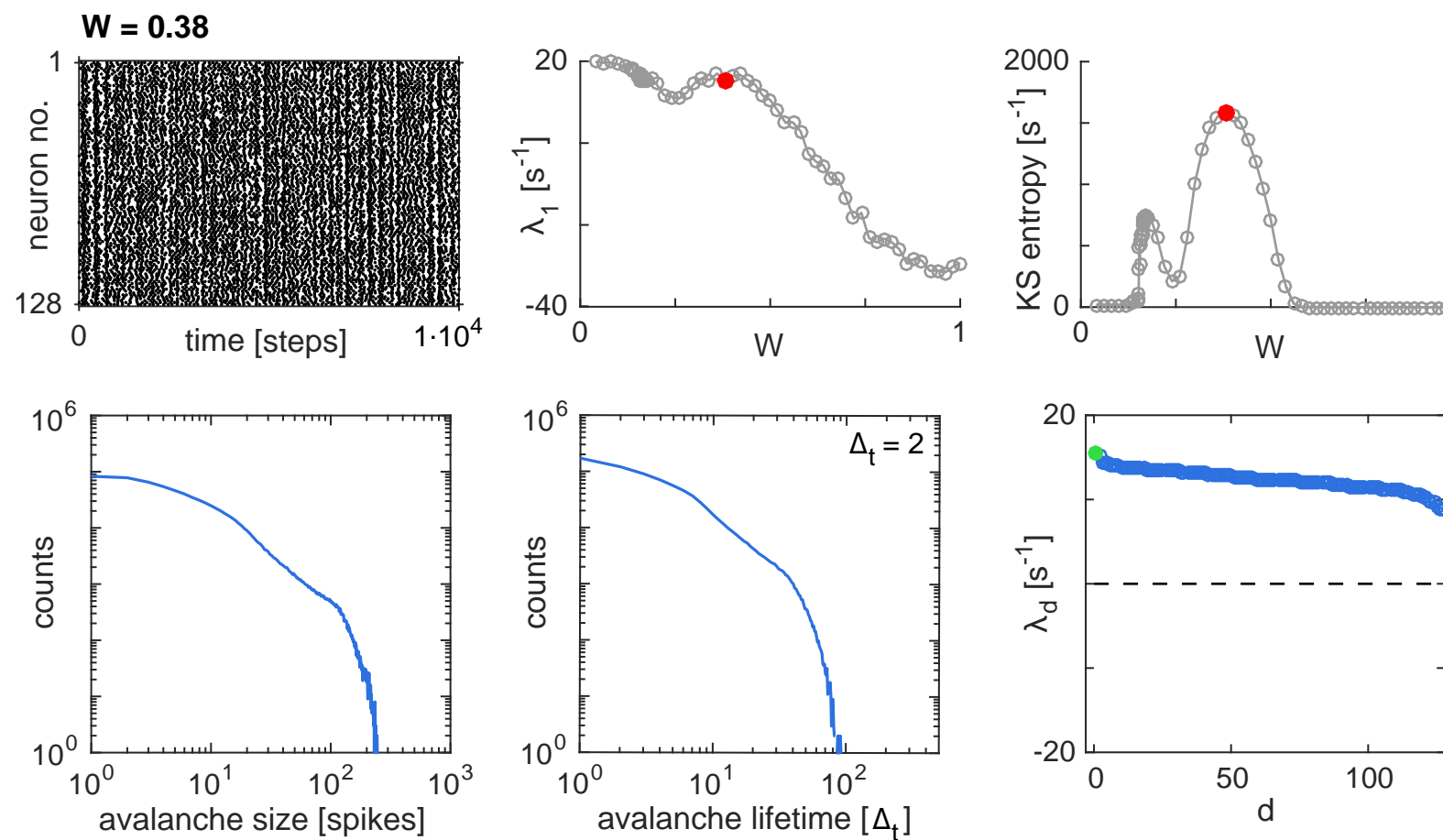
Emergence of preferred patterns at $W = 0.22$, visible in the avalanche distributions.

W=0.3



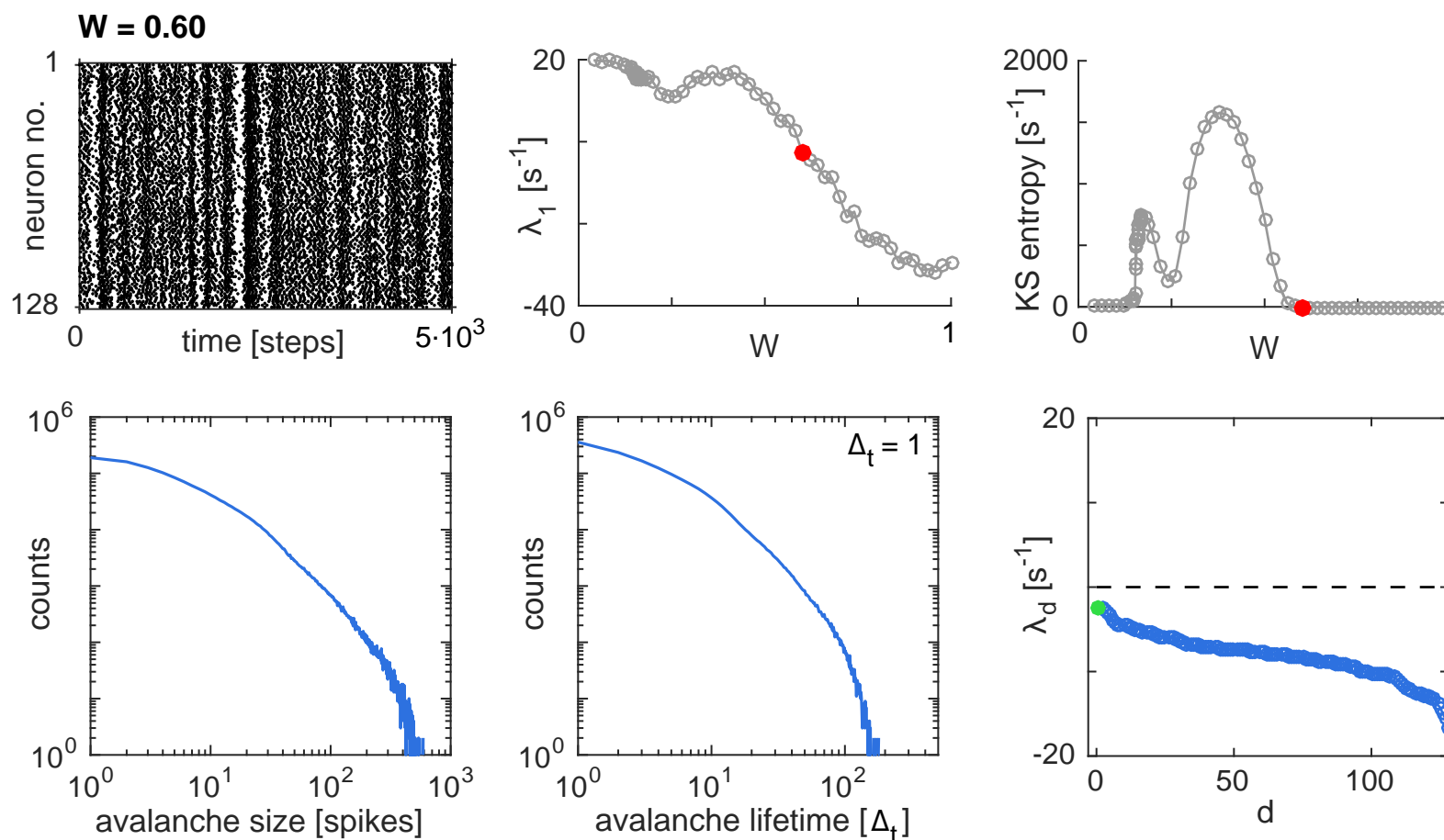
Increase of the largest exponent again; following exponents are dragged to more positive values.
The first exponent still leads the rest of the exponents. Beginning of the fully developed network firing phase.

W=0.38



Second local maximum of the Kolmogorov-Sinai entropy, based on a temporally extended firing pattern phase.
The first Lyapunov exponent has fully merged with the bulk of the remaining positive exponents.
End of the fully developed network firing phase

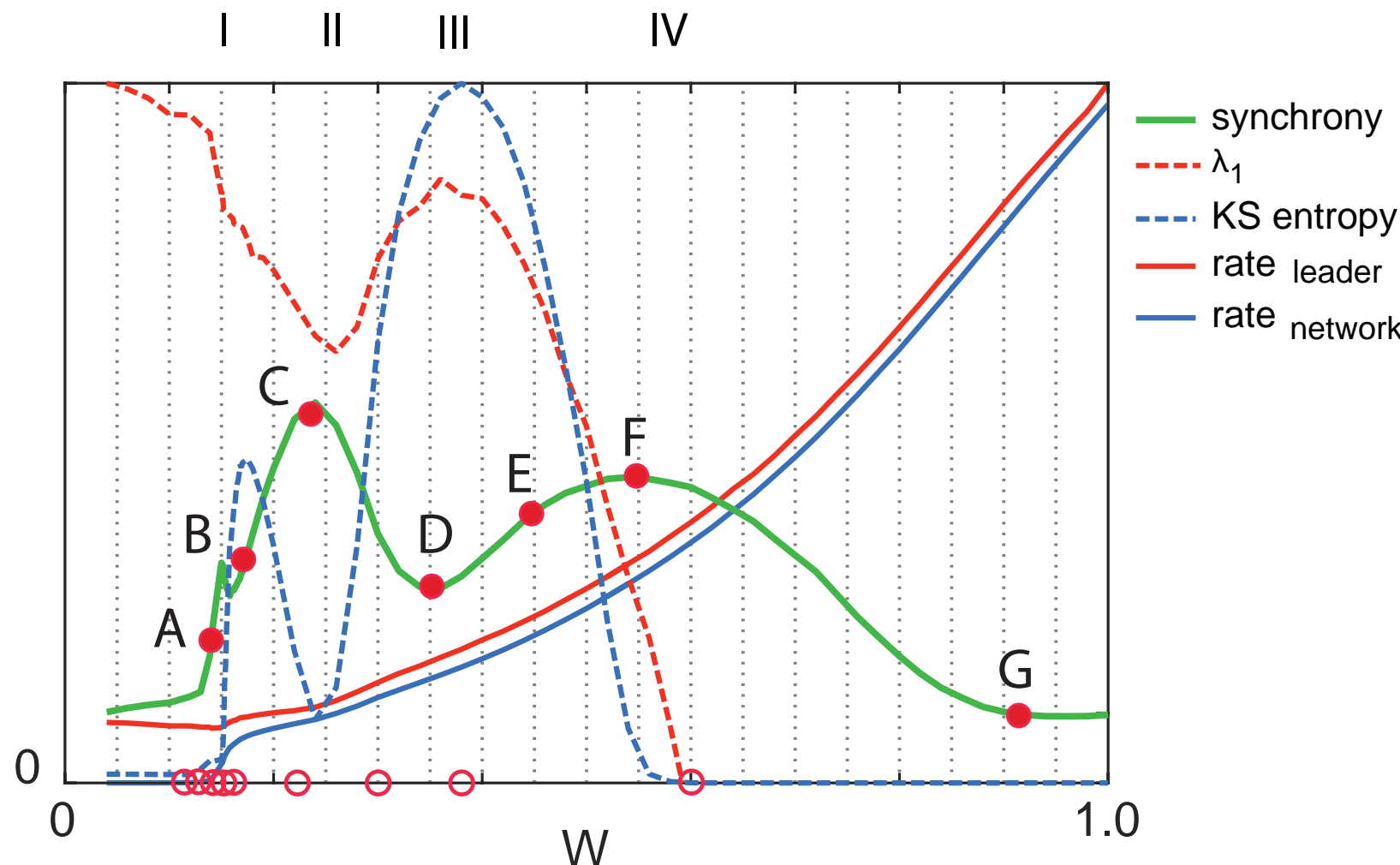
W=0.60



No positive Lyapunov exponents survive at a local maximum of synchronization.

At the transition point from positive to negative leading Lyapunov exponent, the avalanche distribution is very similar to the one presented. Although a small linear slope part is exhibited, the distribution properties rule out avalanche criticality with high confidence.

overview



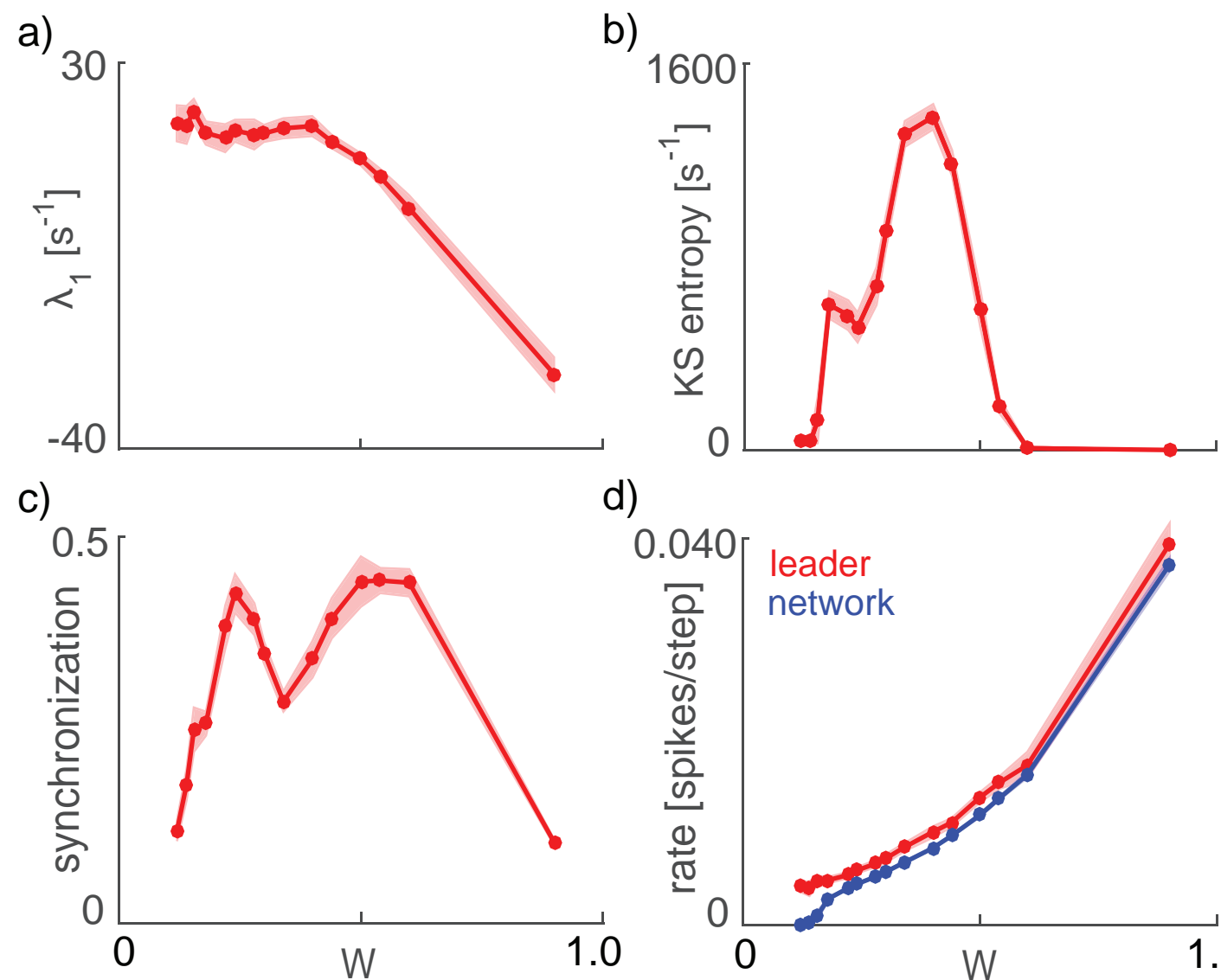
Different network characterizations compiled (y-axis: arbitrary units).

Avalanche criticality is characterized as the unique point where synchronization and KS-entropy increase dramatically, and where the leader neurons merge with the network.

full red dots: Parameter locations corresponding to the raster plots

open red dots: Location of the W -parameters of the network states discussed in detail

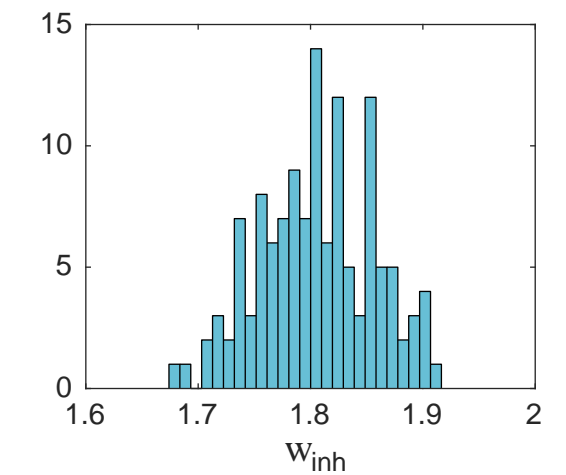
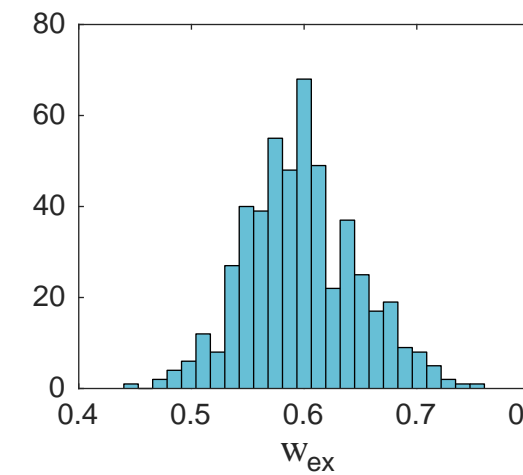
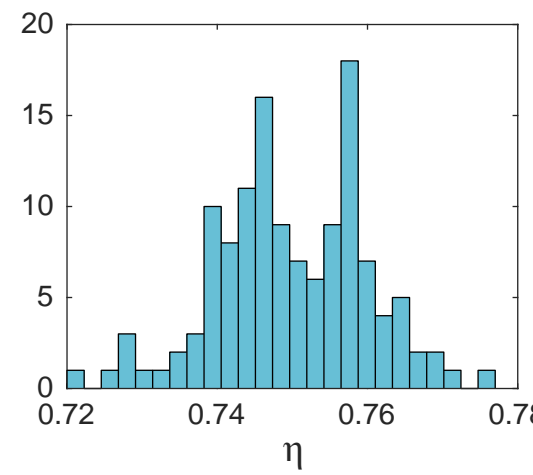
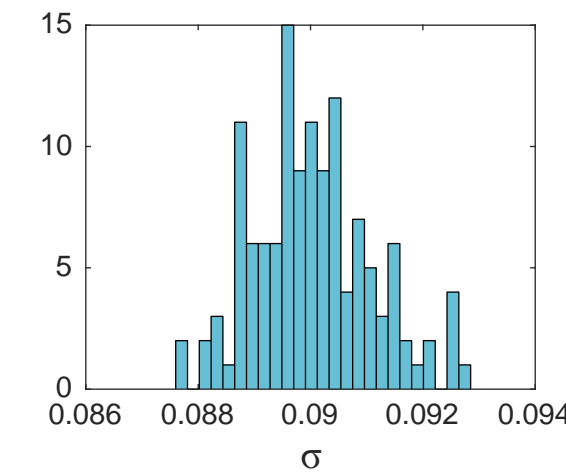
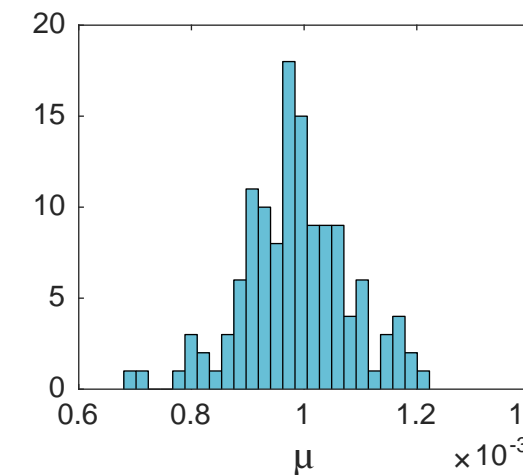
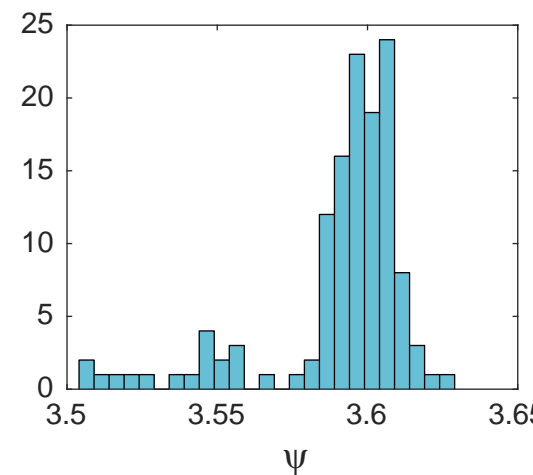
ensemble results



Data points are results averaged over 10 network realizations; shaded area indicate one standard deviation around the mean.

Each simulation for every value of W had a different network adjacency matrix and a different sampling of the random parameters.

ensemble sampling



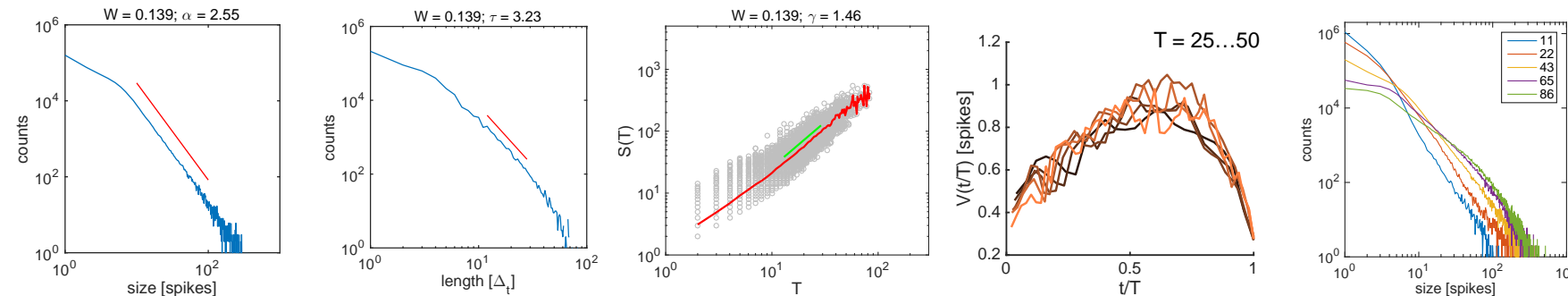
Parameters were sampled from normal distributions $N(mean, variance)$: $\sigma = N(0.09, 10^{-6})$, $\eta = N(0.75, 10^{-4})$, $w_{ex} = w_{ext} = N(0.6, 0.0025)$, $w_{inh} = N(1.8, 0.0025)$, $\mu = N(0.001, 10^{-8})$.

“Leader” neuron’s parameter σ was sampled from $N(0.103, 10^{-6})$. The parameter ψ was sampled from a normal distribution $\psi = N(3.6, 10^{-4})$.

To implement a larger variation among the intrinsically silent neurons, 20% of the ψ values were replaced by samples from a uniform distribution over the interval $\psi \in (3.5, 3.6)$. Similar effect could have been achieved by sampling smaller σ values.

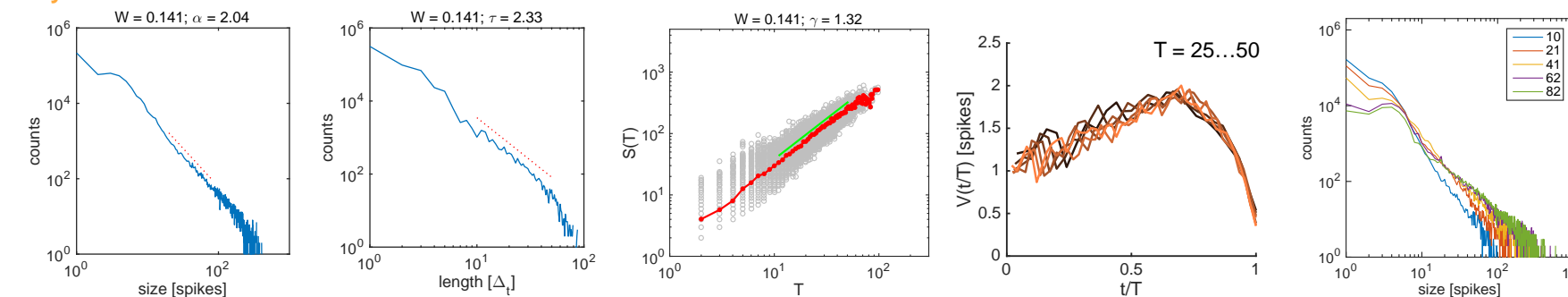
model variations

both inputs



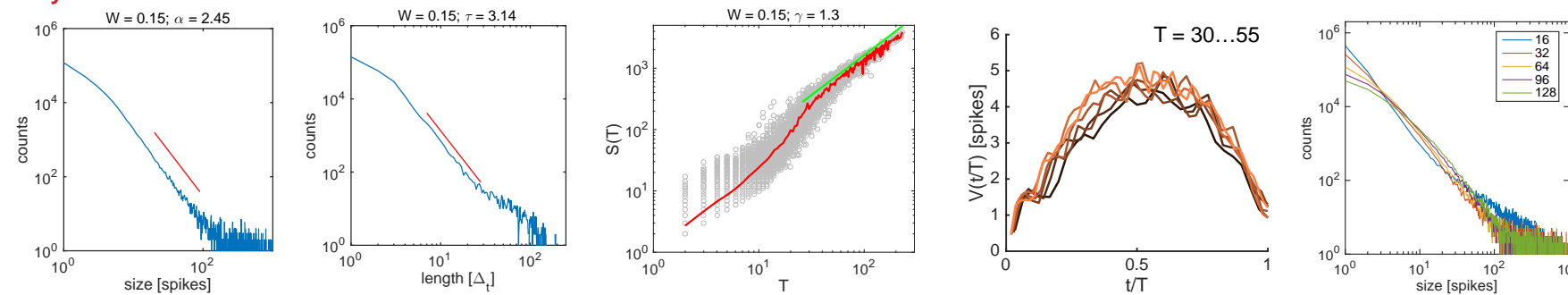
both

only internal



internal only

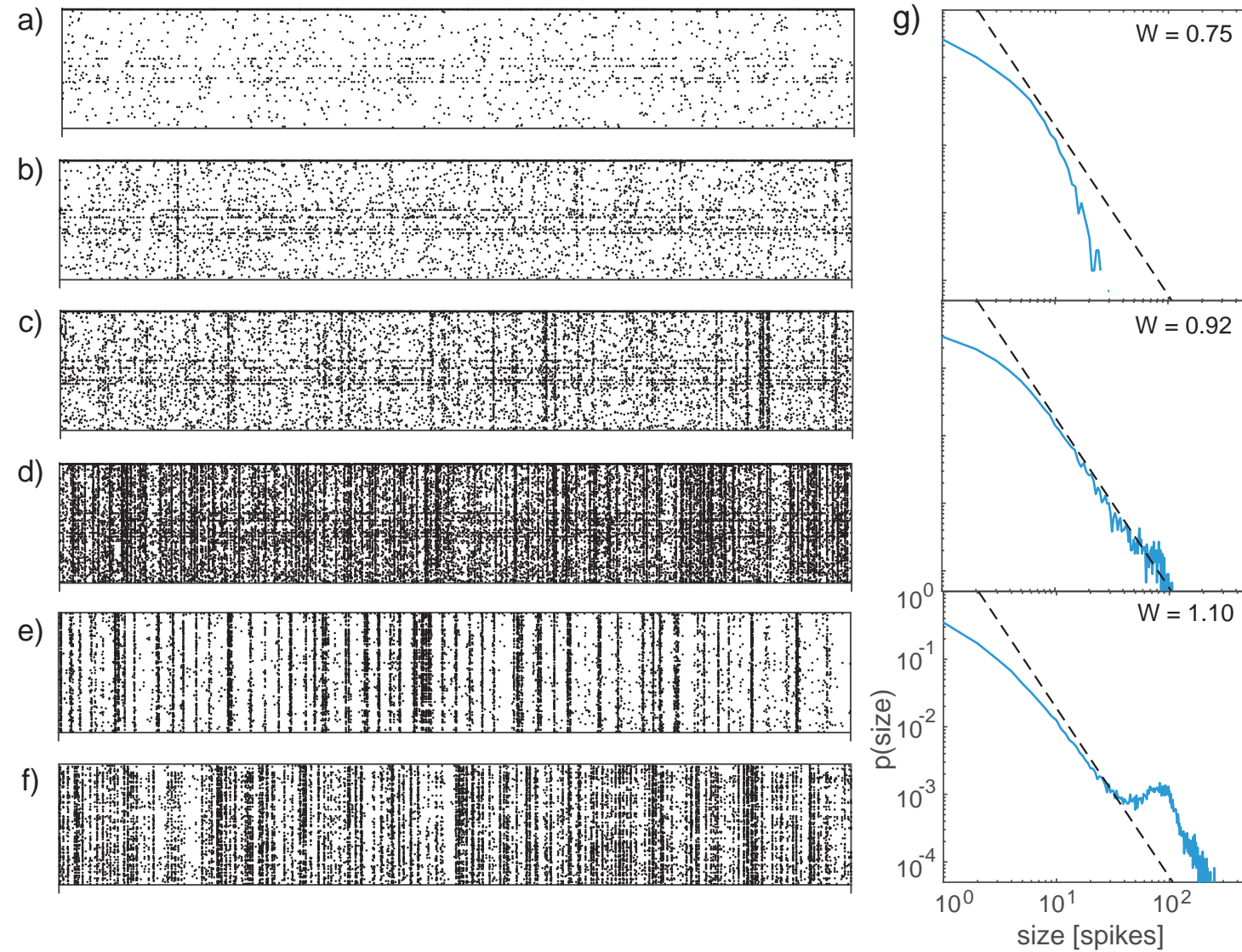
only external



external only

Size distribution, lifetime distribution, size vs. lifetime, shape collapse, temporal binning test (5 realizations)
 $(\Delta_t = 43, 41 \text{ and } 64 \text{ time steps})$.

simpler node dynamics: leaky integrate & fire



a)-f) Raster plots for $W = 0.75, 0.85, 0.9, 1.0, 1.15, 1.7$ (top to bottom).

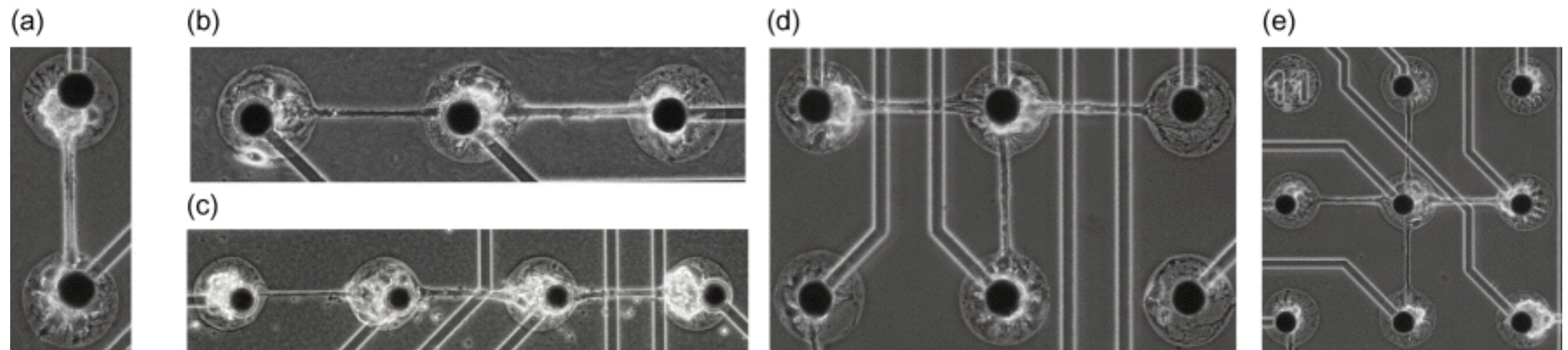
g) Avalanche size distributions. Dashed line: power-law with exponent $\alpha = 2.47$, from a fit at $W = 0.92$ (range of fit = 7 . . . 70; p-value = 0.054).

Temporal binning with bin size equal to the average inter-event interval; pooled data over 10 network realizations.

simpler node dynamics: leaky integrate & fire

- Leaky integrate-and-fire network exhibits a critical point (power-law exponent of $\alpha \approx 2.5$)
- Transition emerges at a changed value of W because of the different sensitivity to inputs of the maps
- Approaching the critical point is accompanied with the emergence of population-sized bursts. These bursts are responsible for the persistent hump that develops at the tail of the distributions at larger values of W
- The network undergoes a structural transformation paradigm that has some similarity to that of the Rulkov dynamics albeit differences in the precise nature of these transformations are expected

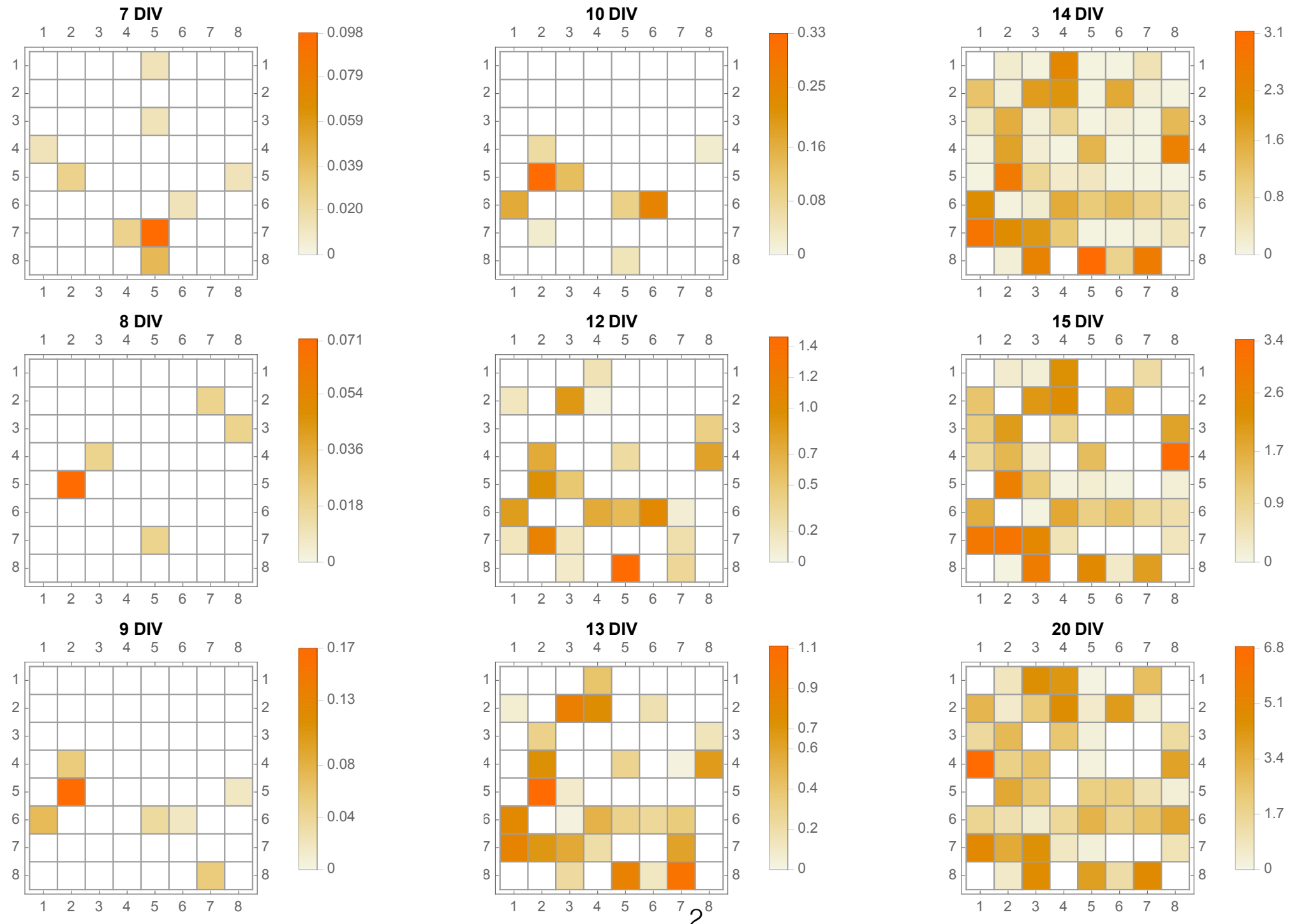
grammatical analysis of MEA spiking data



Hippocampi micro-surgically separated from E18 (embryonic day 18) Sprague- Dawley rats (Koatech Republic of Korea); culture put on MEA-chip (59 electrodes)

(Yoonkey Nam Lab, KAIST)

grammatical analysis of MEA spiking data



(Yoonkey Nam Lab, KAIST)

grammatical analysis: statistical string characterization (nsymb =64)

Walk-through probability:

$$P_{\text{through}}(x) = P_{\text{in}}(x) \cdot P_{\text{out}}(x)$$

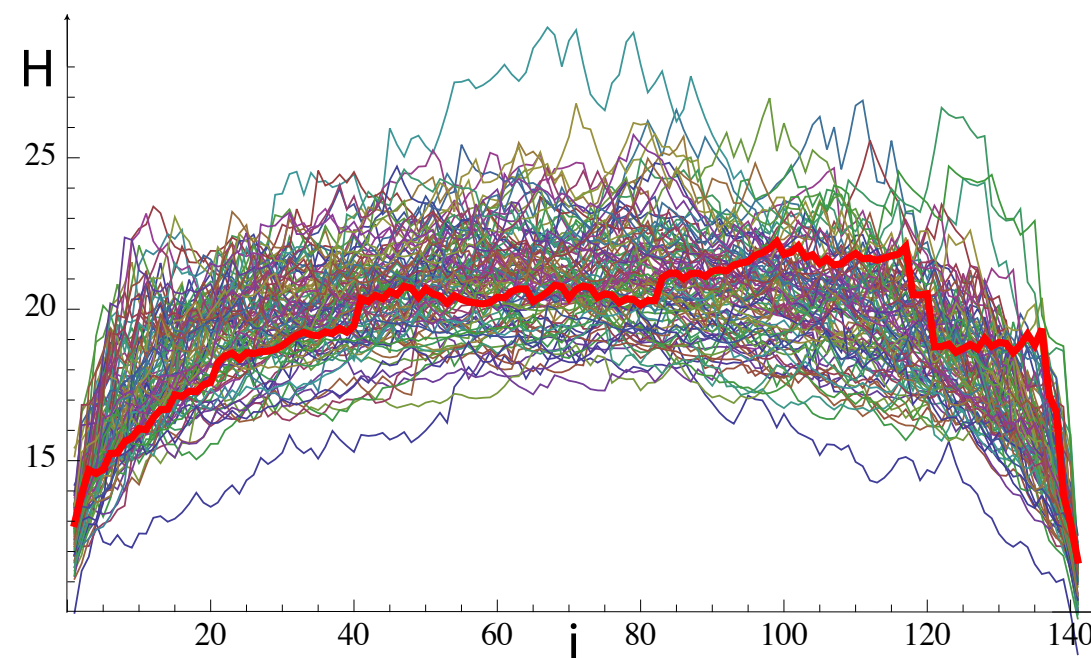
$$P_{\text{in}}(x) = \frac{n!}{n_1! \cdot \dots \cdot n_{n_{\text{symb}}}!} \cdot p_1^{n_1} \cdot \dots \cdot p_n^{n_{n_{\text{symb}}}}$$

$$P_{\text{out}}(x) = \frac{(N - n)!}{(N_1 - n_1)! \cdot \dots \cdot (N_{n_{\text{symb}}} - n_{n_{\text{symb}}})!} \cdot p_1^{(N_1 - n_1)} \cdot \dots \cdot p_n^{(N_{n_{\text{symb}}} - n_{n_{\text{symb}}})}$$

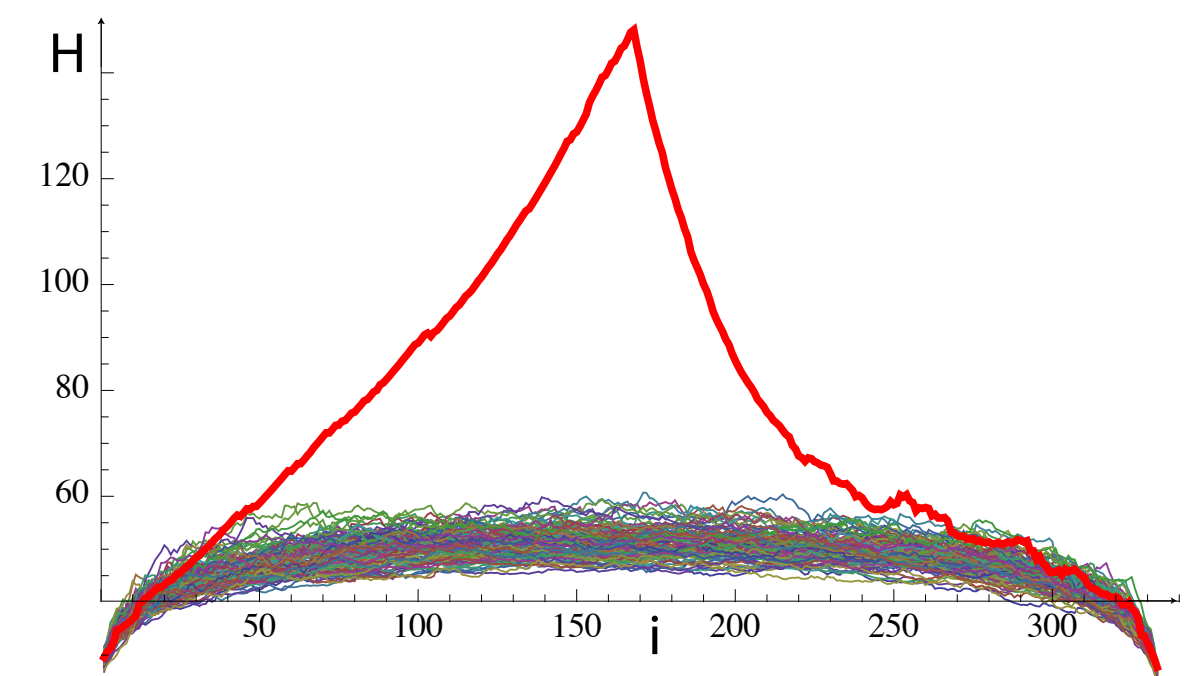
Walk-through entropy H :

$$H_{\text{through}}(\omega) = -\frac{\log(P_{\text{through}}(\omega))}{L} := -\frac{1}{L} \sum_{i=1}^L \log(P_{\text{through}}(x_i)) =: \frac{1}{L} \sum_{i=1}^L H_{\text{through}}(x_i)$$

surrogate t-3 random walks (length-conditioned)

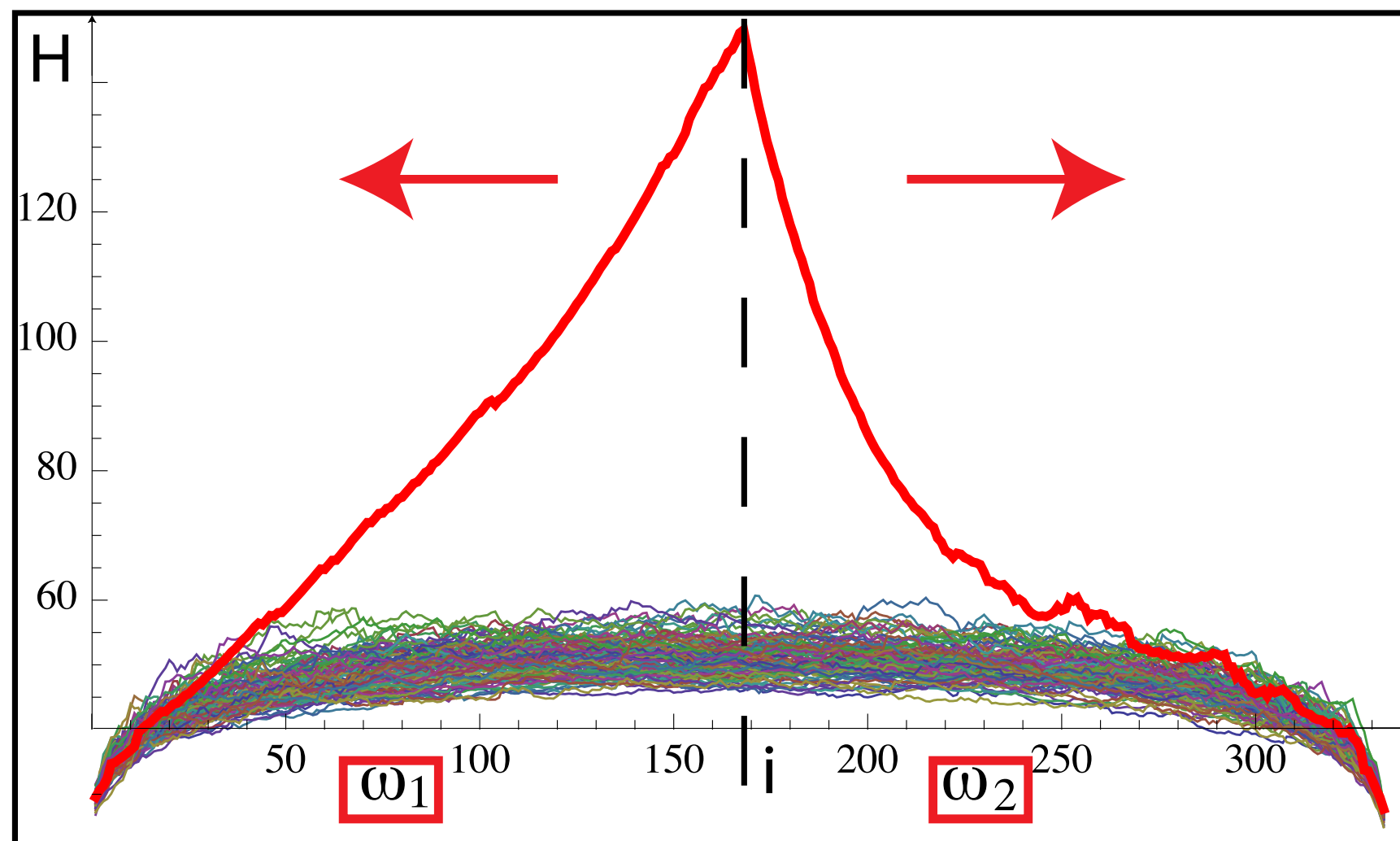


t-3: good model



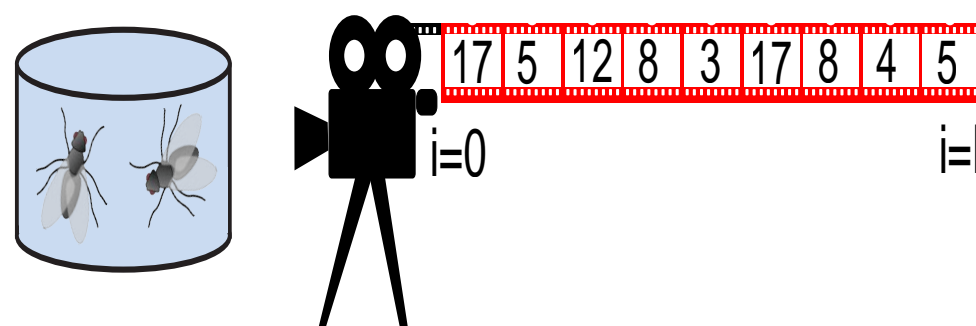
t-3: failure

string separation

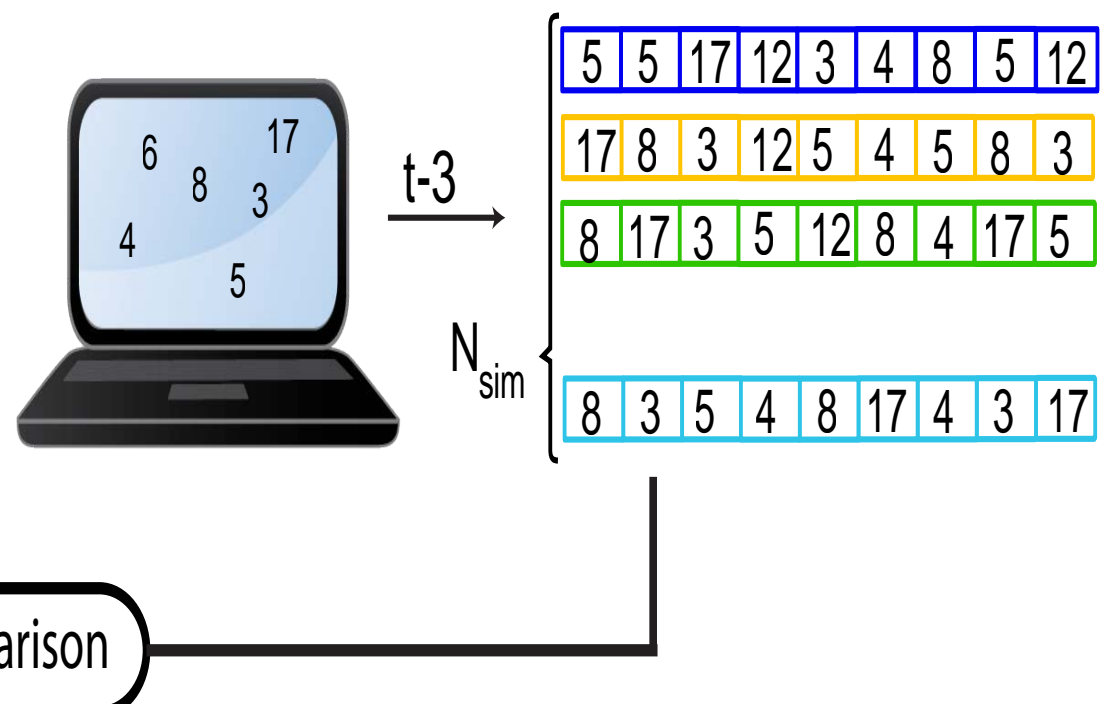


experimental string

A

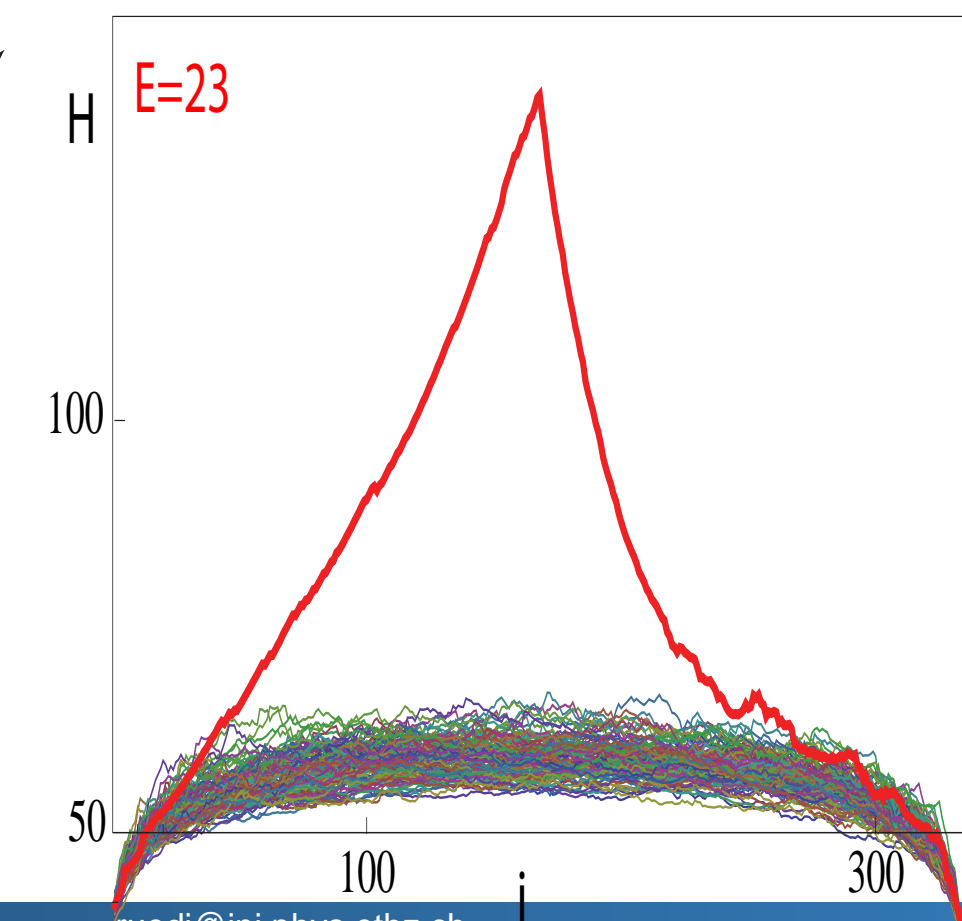
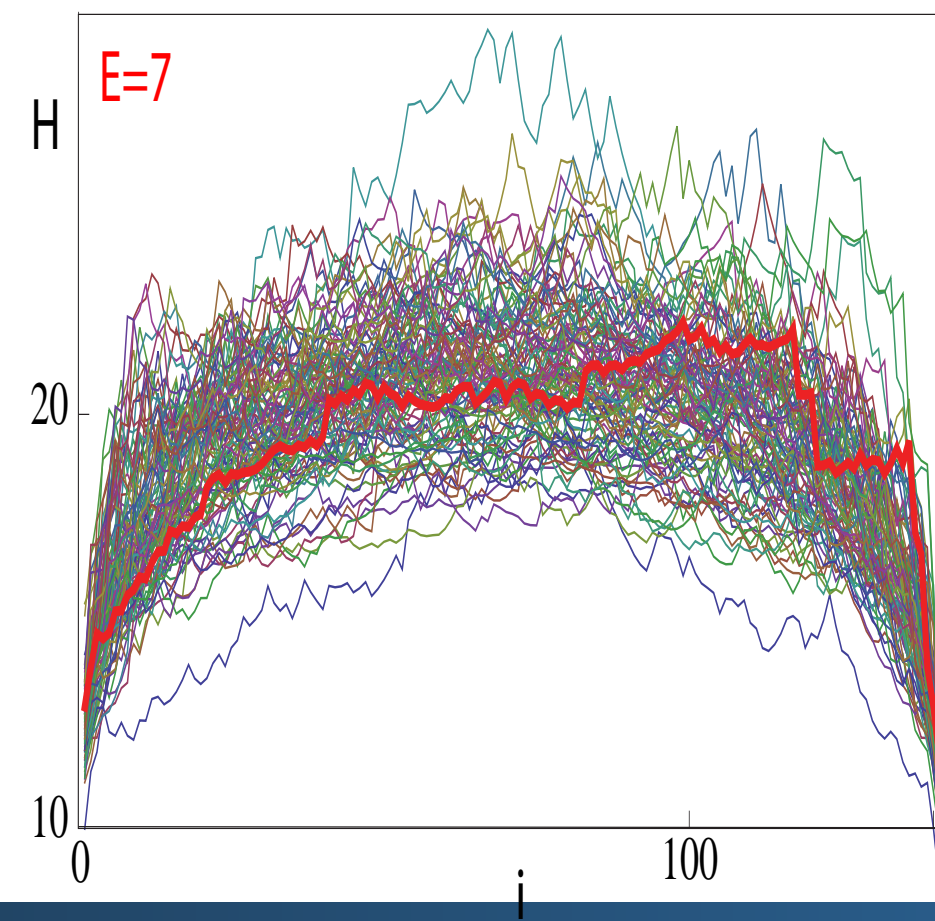


t-3 random walk simulations

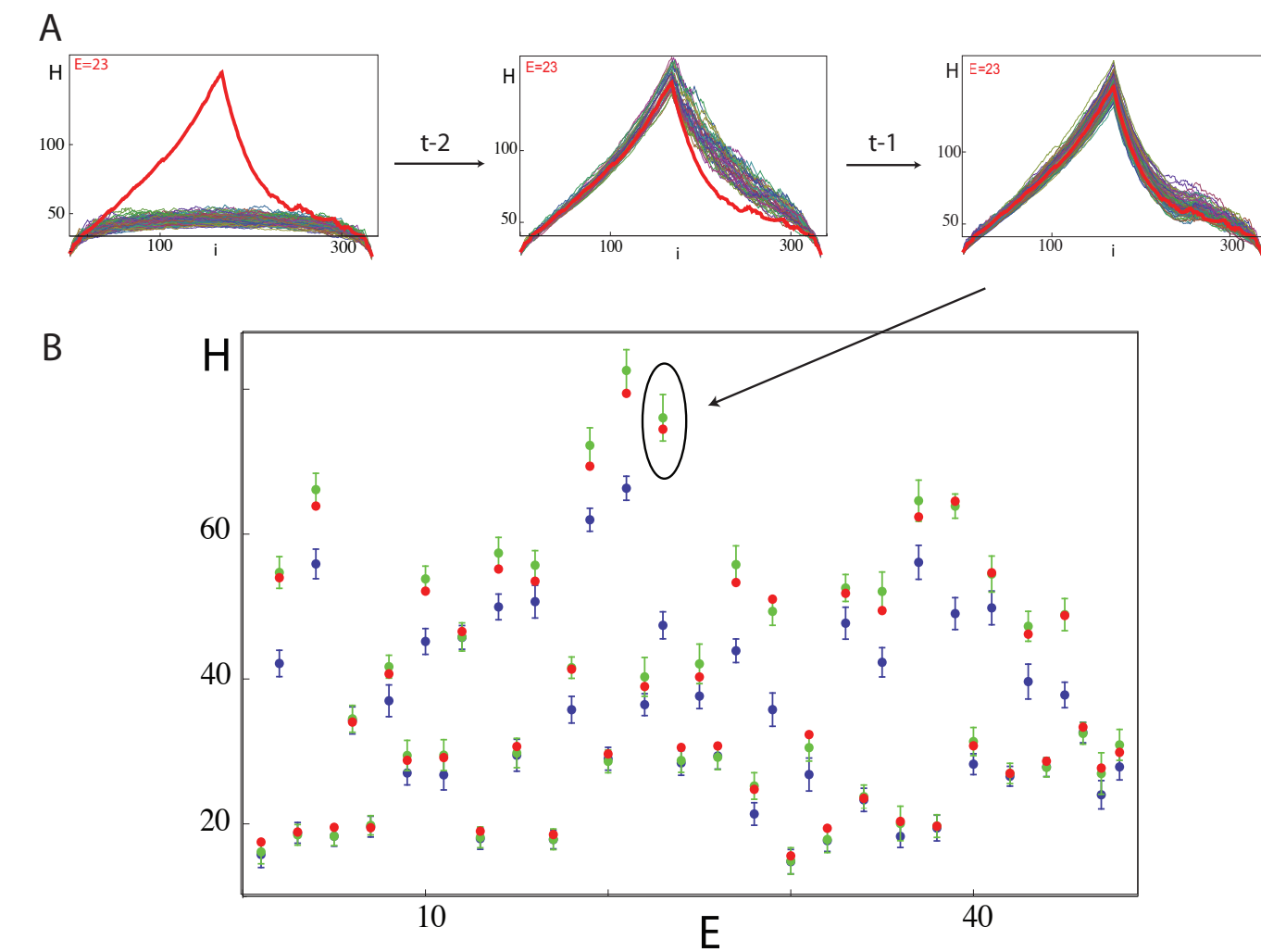


comparison

B

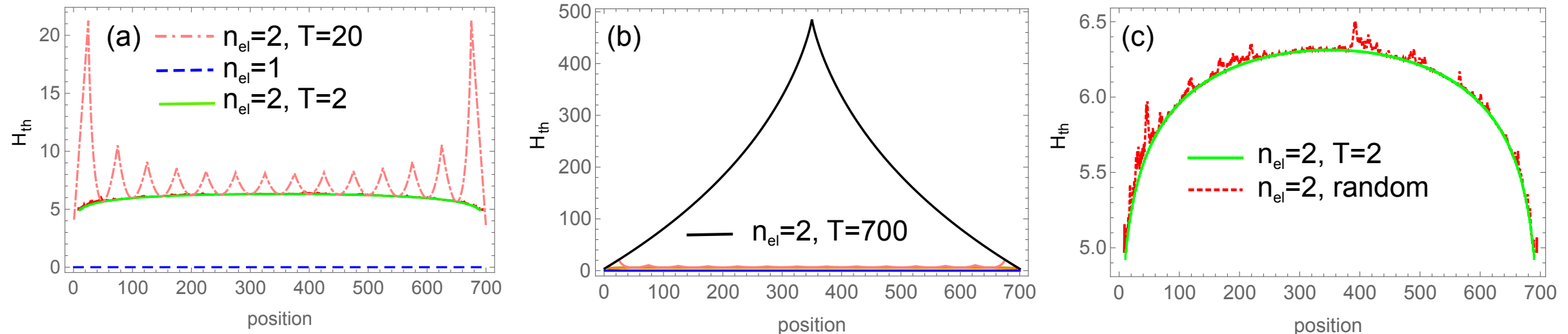


Drosophila precopulatory courtship language



- Generally accepted: spoken human languages fall highest into type t-2 (with Swiss-German of the highest grammatical complexity, Shieber)
- Drosophila's body language is of no lower grammatical complexity than human spoken language

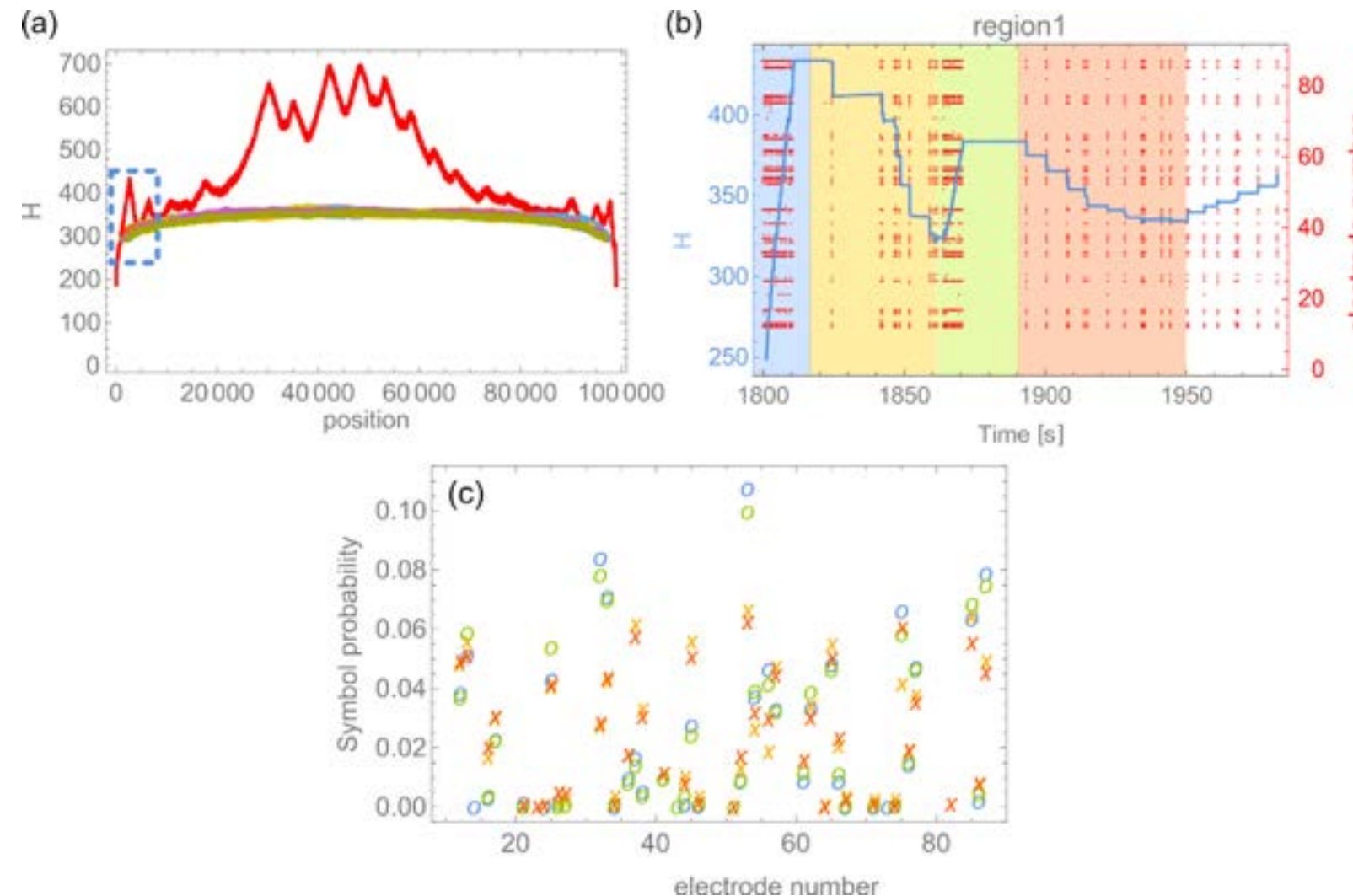
grammatical analysis of MEA spiking data



Entropy H_{th} versus position, evaluated for artificial strings with n_{el} active electrodes and periodicity T :

- a) a single active electrode, $\omega = \{a\}^\infty$ ($n_{el} = 1$, blue dashed line),
- two active electrodes with periodicity of two, $\omega = \{a, b\}^\infty$ ($n_{el} = 2$, $T = 2$, green solid line).
- b) Two active electrodes with periodicity 20 ($n_{el} = 2$, $T = 20$, ochre dashed line) and 700 ($n_{el} = 2$, $T = 700$, black solid line).
- c) Random walk model with two active electrodes ($n_{el} = 2$, random firing, red dashed line).

grammatical analysis of MEA data



- a) Entropy H_{th} versus position for experimental data at 22 DIV (thick red line) and 10 surrogate random walks (colored lines).
- b) Resolved time window, from $t = 1800$ s to 1985 (entropy: blue, l.-h.-s. axis and raster plot: red, r.-h.-s. axis).
- c) Symbol probabilities for the four regions of b).

..entirely different from all what we expect from our modeling approaches!

conclusion

- demonstrated generic non-occurrence of avalanche and edge of chaos criticality
- unexpected stable network transformation paradigm in close to biology networks (ensemble property)
- largely preserved also by simpler node dynamics
- precise nature of the transformations visible in terms of the descriptors showing interaction of coupling, synchronization, chaos amplification and reduction
- *..we may suspect a generic underlying paradigm ..*
- close-to-biology modeling is promising:
in experiments on neural tissue, the strength of neuronal coupling can be manipulated across a similar range

..however: function <-> topology (Soriano)